AD. 400 284

PAUL WEIDLINGER, *Consulting Engineer*
770 Lexington Avenue, New York 21, New York

FORCED VIBRATIONS OF AN ELASTIC CIRCULAR CYLINDRICAL BODY OF FINITE LENGTH SUBMERGED IN AN ACOUSTIC FLUID

PART II—COMPUTATIONAL PROCEDURES AND NUMERICAL EXAMPLE

by

MELVIN L. BARON and ALVA T. MATTHEWS

Office of Naval Research
Project NR 064-464
Contract Nonr 3454(00)FBM
Technical Report No. 2

January 1963

FORCED VIBRATIONS OF AN ELASTIC CIRCULAR CYLINDRICAL BODY OF FINITE LENGTH SUBMERGED IN AN ACOUSTIC FLUID.

Part II - Computational Procedures and Numerical Example.

TABLE OF CONTENTS.

LIST OF SYMBOLS*)

r,θ,z	-	Cylindrical coordinates locating source points, see Fig. (A-1).
$\bar{r},\alpha,\bar{z}$	-	Cylindrical coordinates locating field point, see Fig. (A-1).
u,v,w	-	Longitudinal, tangential and radial displacements of the cylindrical shell.
a	-	Radius of cylinder.
$\bar{a}$	-	Radius of small circle approximation.
C	-	Source strength coefficient per unit of circumferential length for acoustic fluid ($in^2/sec.$).
c_1	-	Velocity of dilatational waves in elastic cylinder.
c_2	-	Velocity of shear waves in elastic cylinder.
c	-	Velocity of sound in water.
G,H,L	-	Source strength coefficients per unit of circumferential length for elastic solid (in^2).
i	-	Source band index.
j	-	Field point index.
$k, k_{1,2,3}$ $\bar{k}, \bar{k}_{1,2,3}$	-	Coefficient $\frac{\omega}{c}$ evaluated for $c = c_1, c_2, c$ as indicated in text; $\bar{k}$ is non-dimensional form $\frac{\omega a}{c}$.
L	-	Length of cylinder.
N	-	Number of bands into which cylinder is divided.
n	-	Number of circumferential waves in the cylinder displacements.

*) Additional symbols are defined as they occur in the text.

p	-	Pressure in fluid (lb/in^2).
P	-	Expansion coefficient of externally applied normal traction to cylinder (lb/in^2).
R	-	Distance between field point and source point,
R_c	-	See Eq. (III-16).
R_o	-	Distance between field point and origin.
$\bar{s}_\alpha$, $\bar{s}_\beta$	-	Contribution of small circle of distributed sources, see Appendix C of Reference [1].
t	-	Time.
X	-	Computational variable.
α_{nji} , β_{nji} , γ_{nji}	-	Integral coefficients of source strengths.
λ, μ	-	Elasticity constants of cylinder.
ϕ	-	Potential function associated with velocities of acoustic fluid.
φ, ψ, η	-	Potential functions associated with displacements of elastic cylinder.
ψ	-	Angle between field and source points, see Fig. (A-1).
ρ_f	-	Mass density of fluid.
ρ, $\bar{\rho}$	-	Non-dimensional variables in radial direction.
ξ, $\bar{\xi}$	-	Non-dimensional variables in z direction.
σ_{rr} , $\sigma_{\theta\theta}$, σ_{zz} $\sigma_{r\theta}$, σ_{rz} , $\sigma_{z\theta}$	-	Cylinder stresses.
$\bar{\theta}$	-	Angle locating small circle of distributed sources, see Fig. (C-1).

ω - Frequency of vibration.

ξ - Slope of R_o, see Fig. (5).

NOTE: r or s appearing as a superscript for the coefficients α_{nji}, β_{nji}, γ_{nji} denotes differentiation with respect to the particular variable used. Dots indicate differentiation with respect to time.

I INTRODUCTION.

The theoretical work and analytical procedures leading to the evaluation of the pressure and velocity fields produced in an acoustic fluid by the forced vibrations of an elastic circular cylindrical body of finite length which is submerged in the fluid have been presented in Reference [1] [1]. The application of the theory to problems of practical interest is discussed in the present report and numerical results are presented for a sample axi-symmetrical problem, i.e. a case in which the cylinder excitation is independent of θ and the response is given by the $n = 0$ component only. For convenience, specific formulas in computational form are given and the major computations are summarized by flow charts. In the sections which follow, it is assumed that the reader is familiar with the material contained in [1] and that all unprefixed formula numbers [2] and section designations refer to the material in that report.

A potential theory approach was used in [1] to evaluate the pressure and velocity fields in the fluid due to the time-harmonic excitation of a submerged cylindrical body of finite length. The stresses and velocities in the elastic cylinder were expressed in terms of three displacement potential functions, each of which satisfies the wave equation. Similarly, the corresponding fluid quantities were expressed in terms of a single fluid velocity potential. Each of the four potential functions were considered to be caused by a group of simple sources of unknown strength which were distributed over the boundaries of the elastic body and the fluid surface at the cylinder-fluid interface. A finite difference approach

---

1) "Forced Vibrations of an Elastic Circular Cylindrical Body of Finite Length Submerged in an Acoustic Fluid", by M.L. Baron, A.T. Matthews and H.H. Bleich, Paul Weidlinger, Consulting Engineer, Office of Naval Research Project NR064-464, Contract 3454(00)FBM, Technical Report No. 1, June 1962.

2) The numbering of formulas in this report will be prefixed by the section number e.g. Eq. (III-1).

was used in which the boundary of the fluid-cylinder interface was divided into a series of bands. On each band, the unknown source strengths were considered to be constant. Conditions on the stresses and velocities at the fluid-elastic body interface gave rise to a system of simultaneous linear algebraic equations on the source strengths. The coefficients in these equations are definite integrals which are evaluated numerically by suitable quadrature formulas for a given geometry and forcing frequency.

In order to solve the coupled forced vibrations problem for arbitrary excitations, the time-harmonic exciting forces were expanded into a Fourier series in θ around the circumference of the cylinder. In this manner, each term corresponding to n, the number of circumferential waves in the particular component, could be treated separately.

The solution of these problems inherently involves a major computational effort directed towards the evaluation of large systems of linear simultaneous algebraic equations on the source strength coefficients. If the cylinder-fluid interface is divided into N bands, sets of 8N ($n \neq 0$) and 6N ($n = 0$) simultaneous equations are obtained. It will be shown that in each case, the computations can be reduced to the evaluation of a number of systems of 2N equations. For the application of the theory to practical problems in which as many as 50 or more bands might be considered, large electronic computers capable of solving systems of one to two hundred linear equations would be required.

Section II of this report gives the procedures and detailed formulas for the evaluation of the $n \neq 0$ response components. Section III gives similar information for the axi-symmetrical case, $n = 0$, and includes an illustrative numerical example for a case with the parameter ratios $\frac{L}{a} = 2$ and $\frac{\omega a}{c} = 2.01$.

It is felt that the present theory may find useful applications in evaluating the response in a fluid due to the harmonic excitation of large transducers. In addition, current work on the extension of this approach to the case of thick walled elastic shells submerged in an acoustic fluid, is under way.

II COMPUTATIONAL PROCEDURES, $n \neq 0$.

This section describes the computational procedures for the evaluation of the source strength coefficients on the cylinder-fluid interface and the subsequent evaluation of the pressure and velocity fields in the acoustic fluid. The formulas on the real and imaginary parts of the source strength coefficients are presented in a form particularly suitable for computations. The computational procedure is conveniently divided into three major portions [3] : a) Evaluation of the coefficients α_{nji} , β_{nji} and γ_{nji} and their space derivatives, using Eqs. (29), (30) and Eqs. (45)-(52); b) Solution of Eqs. (80)-(87) for the source strength coefficients G_{ni} , H_{ni} , L_{ni} and C_{ni} ; and c) Evaluation of the pressure and/or the velocity field in the fluid, using Eqs. (67)-(69) and Eqs. (89)-(89a).

For a particular set of input parameters, i.e. the cylinder geometry; the elastic constants of the cylinder material; the fluid constants; and the space distribution of the time-harmonic excitation, the cylindrical shell is divided into a number N of subdivisions and the computations are started. The number N of bands on the shell-fluid interface which are chosen for any particular problem will depend essentially on the complexity of the applied excitation and the accuracy required in the results.

The evaluation of the coefficients α_{nji} , β_{nji} , γ_{nji} and their space derivatives have been described in detail for the $n = 0$ case in Section (IV) of Reference [1] and no further amplification is required here. The computational formulas for the real and imaginary parts of these coefficients for $n \neq 0$ are given in Appendix A of this paper for the two cases, $i = j$ and $i \neq j$.

---

3) See Reference [1], Section IV, Pg. 37 ff.

The second major computational effort is the evaluation of the complex source strengths G_{ni} , H_{ni} , L_{ni} and C_{ni} . With four such complex unknown coefficients for each band N on the cylinder-fluid interface, this leads to a system of 8N simultaneous linear algebraic equations on the real and imaginary parts of the source strengths [4]. For the axisymmetrical case n = 0, all the coefficients L_{0i} are zero and a system of 6N equations is obtained.

The source strengths and the coefficients α_{nji} , β_{nji} , γ_{nji} and their space derivatives appearing in Eqs. (80)-(87) are written in terms of their real and imaginary parts, e.g.

$$G_{ni} = \bar{G}_{ni} + i\,\bar{\bar{G}}_{ni}$$

$$\alpha_{ni} = \bar{\alpha}_{ni} + i\,\bar{\bar{\alpha}}_{ni}$$

and the real and imaginary parts of each of Eqs. (80)-(87) are equated, thus leading to the following set of equations in computational form [5]:

Point j on the surface r = a

$$\mathrm{Re}\,\sigma_{rr} = \sum_{i=1}^{N}\Big\{\bar{G}_{ni}\bar{d}_1 - \bar{\bar{G}}_{ni}\bar{\bar{d}}_1 + \bar{H}_{ni}a\bar{d}_2 - \bar{\bar{H}}_{ni}a\bar{\bar{d}}_2 + \bar{L}_{ni}\bar{d}_3 - \bar{\bar{L}}_{ni}\bar{\bar{d}}_3 + \bar{C}_{ni}\bar{d}_4 + \bar{\bar{C}}_{ni}\bar{\bar{d}}_4\Big\}_{r=a} = P_{rr,nj} \qquad \text{(II-1)}$$

---

4) Recent developments in the programming of systems of simultaneous linear algebraic equations with complex unknowns may allow the direct evaluation of the complex source strengths G_{ni} , H_{ni} , L_{ni} and C_{ni} without breaking them into their real and imaginary parts. This would reduce the problem to the solution of systems of 4N ($n \neq 0$) and 3N ($n = 0$) equations respectively.

5) In the formulas which follow, the subscript nji in each of the d coefficients will be understood, e.g. $d_2 = d_{nj12}$ etc.

$$\text{Im } \sigma_{rr} = \sum_{i=1}^{N} \Big\{ \bar{G}_{ni} \bar{d}_1 + \bar{\bar{G}}_{ni} d_1 + \bar{H}_{ni} a \bar{d}_2 + \bar{\bar{H}}_{ni} a d_2 + L_{ni} \bar{d}_3 + \bar{L}_{ni} d_3 - \bar{C}_{ni} d_4 - \bar{\bar{C}}_{ni} \bar{d}_4 \Big\}_{r=a} = 0 \qquad \text{(II-2)}$$

$$\text{Re } \sigma_{rz} = \sum_{i=1}^{N} \Big\{ \bar{G}_{ni} d_5 - \bar{\bar{G}}_{ni} \bar{d}_5 + \bar{H}_{ni} a d_6 - \bar{\bar{H}}_{ni} a \bar{d}_6 + L_{ni} d_7 - \bar{L}_{ni} \bar{d}_7 \Big\}_{r=a} = 0 \qquad \text{(II-3)}$$

$$\text{Im } \sigma_{rz} = \sum_{i=1}^{N} \Big\{ \bar{G}_{ni} \bar{d}_5 + \bar{\bar{G}}_{ni} d_5 + \bar{H}_{ni} a \bar{d}_6 + \bar{\bar{H}}_{ni} a d_6 + L_{ni} \bar{d}_7 + \bar{L}_{ni} d_7 \Big\}_{r=a} = 0 \qquad \text{(II-4)}$$

$$\text{Re } \sigma_{r\theta} = \sum_{i=1}^{N} \Big\{ \bar{G}_{ni} d_8 - \bar{\bar{G}}_{ni} \bar{d}_8 + \bar{H}_{ni} a d_9 - \bar{\bar{H}}_{ni} a \bar{d}_9 + L_{ni} d_{10} - \bar{L}_{ni} \bar{d}_{10} \Big\}_{r=a} = 0 \qquad \text{(II-5)}$$

$$\text{Im } \sigma_{r\theta} = \sum_{i=1}^{N} \Big\{ \bar{G}_{ni} \bar{d}_8 + \bar{\bar{G}}_{ni} d_8 + \bar{H}_{ni} a \bar{d}_9 + \bar{\bar{H}}_{ni} a d_9 + L_{ni} \bar{d}_{10} + \bar{L}_{ni} d_{10} \Big\}_{r=a} = 0 \qquad \text{(II-6)}$$

$$\text{Re } \dot{w} = \sum_{i=1}^{N} \Big\{ - \bar{G}_{ni} \bar{\alpha}^{r}_{nji} - \bar{\bar{G}}_{ni} \alpha^{r}_{nji} + \bar{H}_{ni} a \bar{\beta}^{rz}_{nji} + \bar{\bar{H}}_{ni} a \beta^{rz}_{nji} - L_{ni} \frac{n}{r} \bar{\beta}_{nji} - \bar{L}_{ni} \frac{n}{r} \beta_{nji} + \frac{\bar{C}_{ni}}{\omega} \gamma^{r}_{nji} - \frac{\bar{\bar{C}}_{ni}}{\omega} \bar{\gamma}^{r}_{nji} \Big\}_{r=a} = 0 \qquad \text{(II-7)}$$

$$\text{Im } \dot{w} = \sum_{i=1}^{N} \Big\{ \bar{G}_{ni} \alpha^{r}_{nji} - \bar{\bar{G}}_{ni} \bar{\alpha}^{r}_{nji} - \bar{H}_{ni} a \beta^{rz}_{nji} + \bar{\bar{H}}_{ni} a \bar{\beta}^{rz}_{nji} + L_{ni} \frac{n}{r} \beta_{nji} - \bar{L}_{ni} \frac{n}{r} \bar{\beta}_{nji} + \frac{\bar{C}_{ni}}{\omega} \bar{\gamma}^{r}_{nji} + \frac{\bar{\bar{C}}_{ni}}{\omega} \gamma^{r}_{nji} \Big\}_{r=a} = 0 \qquad \text{(II-8)}$$

Point j on end surfaces, z = 0 and z = L

$$\text{Re } \sigma_{zz} = \sum_{i=1}^{N} \left\{ \bar{G}_{ni} \bar{d}_{11} - \bar{\bar{G}}_{ni} \bar{\bar{d}}_{11} + \bar{H}_{ni} \bar{ad}_{12} - \bar{\bar{H}}_{ni} \bar{\bar{ad}}_{12} + \bar{C}_{ni} \bar{\bar{d}}_{4} + \bar{\bar{C}}_{ni} \bar{d}_{4} \right\}_{z=0,L} = P_{zz,nj} \tag{II-9}$$

$$\text{Im } \sigma_{zz} = \sum_{i=1}^{N} \left\{ \bar{G}_{ni} \bar{\bar{d}}_{11} + \bar{\bar{G}}_{ni} \bar{d}_{11} + \bar{H}_{ni} \bar{\bar{ad}}_{12} + \bar{\bar{H}}_{ni} \bar{ad}_{12} - \bar{C}_{ni} \bar{d}_{4} + \bar{\bar{C}}_{ni} \bar{\bar{d}}_{4} \right\}_{z=0,L} = 0 \tag{II-10}$$

$\text{Re } \sigma_{rz} = 0$ Apply Eq. (II-3) at point.

$\text{Im } \sigma_{rz} = 0$ Apply Eq. (II-4) at point.

$$\text{Re } \sigma_{z\theta} = \sum_{i=1}^{N} \left\{ \bar{G}_{ni} \bar{d}_{13} - \bar{\bar{G}}_{ni} \bar{\bar{d}}_{13} + \bar{H}_{ni} \bar{ad}_{14} - \bar{\bar{H}}_{ni} \bar{\bar{ad}}_{14} - \bar{L}_{ni} \bar{\beta}^{rz}_{nji} + \bar{\bar{L}}_{ni} \bar{\bar{\beta}}^{rz}_{nji} \right\}_{z=0,L} = 0 \tag{II-11}$$

$$\text{Im } \sigma_{z\theta} = \sum_{i=1}^{N} \left\{ \bar{G}_{ni} \bar{\bar{d}}_{13} + \bar{\bar{G}}_{ni} \bar{d}_{13} + \bar{H}_{ni} \bar{\bar{ad}}_{14} + \bar{\bar{H}}_{ni} \bar{ad}_{14} - \bar{L}_{ni} \bar{\bar{\beta}}^{rz}_{nji} - \bar{\bar{L}}_{ni} \bar{\beta}^{rz}_{nji} \right\}_{z=0,L} = 0 \tag{II-12}$$

$$\text{Re } \hat{u} = \sum_{i=1}^{N} \left\{ - \bar{G}_{ni} \bar{\bar{\alpha}}^{z}_{nji} - \bar{\bar{G}}_{ni} \bar{\alpha}^{z}_{nji} + \bar{H}_{ni} \bar{\bar{ad}}_{15} + \bar{\bar{H}}_{ni} \bar{ad}_{15} + \frac{\bar{C}_{ni}}{\omega} \bar{\gamma}^{z}_{nji} - \frac{\bar{\bar{C}}_{ni}}{\omega} \bar{\bar{\gamma}}^{z}_{nji} \right\}_{z=0,L} = 0 \tag{II-13}$$

$$\text{Im } \hat{u} = \sum_{i=1}^{N} \left\{ \bar{G}_{ni} \bar{\alpha}^{z}_{nji} - \bar{\bar{G}}_{ni} \bar{\bar{\alpha}}^{z}_{nji} - \bar{H}_{ni} \bar{ad}_{15} + \bar{\bar{H}}_{ni} \bar{\bar{ad}}_{15} + \frac{\bar{C}_{ni}}{\omega} \bar{\bar{\gamma}}^{z}_{nji} + \frac{\bar{\bar{C}}_{ni}}{\omega} \bar{\gamma}^{z}_{nji} \right\}_{z=0,L} = 0 \ . \tag{II-14}$$

Expressions for the coefficients $\tilde{d}_k$ and $\bar{\tilde{d}}_k$ are given in Table II-1 and the expressions for the real and imaginary parts of the coefficients α_{nji}, β_{nji}, γ_{nji} and their space derivatives are given in Appendix A of this report [See Eq. (A-6) - (A-38)].

The application of Eqs. (II-1)-(II-14) at the points on the fluid-cylinder interface yields the set of 8N simultaneous linear equations on the source strengths. These equations can be solved by either of two approaches:

1) a direct solution of the system of 8N equations on a large electronic computer, or
2) a reduction of the system of 8N equations to a series of 2N systems and their subsequent solution on an electronic computer. These alternatives will be illustrated in detail in Section III of this report in which the illustrative problem for an axisymmetrical problem, n = 0, is presented.

Once the source strength coefficients are evaluated, the complex fluid pressure at a field point j is obtained by direct substitution of the source strength coefficients C_{ni} into Eqs. (89)-(89a):

$$p_{n,j} = \sum_{i=1}^{N} \rho_f \omega e^{i\omega t} \left[- \left(C_{ni} \bar{\gamma}_{nji} + \bar{C}_{ni} \gamma_{nji} \right) + i \left(\bar{C}_{ni} \bar{\gamma}_{nji} - C_{ni} \gamma_{nji} \right) \right] . \qquad \text{(II-15)}$$

The far field pressures in the fluid can be evaluated from the simplified asymptotic expression, Eq. (89a):

$$p_{n,j} = \left[- \frac{i^{n+1} \omega \rho_f \cos n\theta \, e^{i\omega t}}{2} \sum_{i=1}^{N} C_{ni} \bar{r} \, e^{ik_3 \bar{z} \sin \bar{\xi}} \, J_n \left(k_3 \bar{r} \cos \bar{\xi} \right) \right] \frac{e^{- \frac{i\omega R_o}{c}}}{R_o}$$

(II-16)

The use of this asymptotic expression greatly simplifies the numerical computation of the far field fluid pressure, since it eliminates the computation of the γ_{njl} integral coefficients for each point along a specific ray in the fluid. An additional convenience is the fact that once the pressure $p_{n,j}$ has been evaluated from Eq. (II-16) for a given point P_j on the ray specified by R_o and $\bar{\xi}$, it can easily be evaluated for any other point on that ray by changing the scale factor $\frac{e^{-\frac{i\omega R_o}{c}}}{R_o}$, [See Figure III-3].

Table I - Evaluation of the Coefficients $\bar{d}_k$ and $\bar{\bar{d}}_k$ [6]

$$\bar{d}_1 = -\frac{\lambda\omega^2}{c_1^2}\bar{\alpha}_{nji} + 2\mu\bar{\alpha}^{rr}_{nji} \quad ; \quad \bar{d}_2 = -2\mu\bar{\beta}^{rrz}_{nji}$$

$$\bar{d}_3 = 2\mu\left[\frac{n}{r}\bar{\beta}^{r}_{nji} - \frac{n}{r^2}\bar{\beta}_{nji}\right] \quad ; \quad \bar{d}_4 = \rho_f\omega\,\bar{\gamma}_{nji}$$

$$\bar{d}_5 = 2\bar{\alpha}^{rz}_{nji} \quad ; \quad \bar{d}_6 = \left[-2\bar{\beta}^{rzz}_{nji} - \frac{\omega^2}{c_2^2}\bar{\beta}^{r}_{nji}\right]$$

$$\bar{d}_7 = \frac{n}{r}\bar{\beta}^{z}_{nji} \quad ; \quad \bar{d}_8 = \frac{2n}{r^2}\bar{\alpha}_{nji} - \frac{2n}{r}\bar{\alpha}^{r}_{nji}$$

$$\bar{d}_9 = -\frac{2n}{r^2}\bar{\beta}^{z}_{nji} + \frac{2n}{r}\bar{\beta}^{rz}_{nji} \quad ; \quad \bar{d}_{10} = -\bar{\beta}^{rr}_{nji} - \frac{n^2}{r^2}\bar{\beta}_{nji} + \frac{1}{r}\bar{\beta}^{r}_{nji}$$

$$\bar{d}_{11} = -\frac{\lambda\omega^2}{c_1^2}\bar{\alpha}_{nji} + 2\mu\bar{\alpha}^{zz}_{nji} \quad ; \quad \bar{d}_{12} = -2\mu\bar{\beta}^{zzz}_{nji} - 2\mu\frac{\omega^2}{c^2}\bar{\beta}^{z}_{nji}$$

$$\bar{d}_{13} = -\frac{2n}{r}\bar{\alpha}^{z}_{nji} \quad ; \quad \bar{d}_{14} = \frac{2n}{r}\bar{\beta}^{zz}_{nji} + \frac{n\omega^2}{rc_2^2}\bar{\beta}_{nji}$$

$$\bar{d}_{15} = \frac{\omega^2}{c_2^2}\bar{\beta}_{nji} + \bar{\beta}^{zz}_{nji}$$

---

6) The formulas for the coefficients $\bar{\bar{d}}_k$ are obtained by replacing the single bar values by the corresponding double bar values in each case.

III COMPUTATIONAL PROCEDURES AND NUMERICAL EXAMPLE, n = 0.

For illustrative purposes, the following axisymmetrical problem is presented. An elastic cylinder of radius a and length L, immersed in an infinite acoustic fluid, undergoes an electromagnetically induced time - harmonic uniform strain, $\epsilon_{zz} = \epsilon_o e^{i\omega t}$, in the axial direction, while the radial and circumferential strains ϵ_{rr} and $\epsilon_{\theta\theta}$ are kept equal to zero (Fig. III-1a). By superposition, the pressure field that is produced in the fluid by the straining of the cylinder will be equivalent to the fluid pressures produced by a set of fictitious surface tractions which are applied to the solid cylinder in the ratio

$$\frac{\sigma_{rr}}{\sigma_{zz}} = \frac{\lambda}{\lambda + 2\mu} = \frac{\nu}{1 - \nu} \quad . \tag{a}$$

To illustrate this, consider first, the cylinder under the action of applied surface tractions σ_{rr} and σ_{zz} (Fig. III-1b). These tractions are chosen so as to bring the cylinder back to its original unstrained state, i.e.

$$\begin{aligned} \sigma_{rr} &= - \lambda \epsilon_o e^{i\omega t} \\ \sigma_{zz} &= - (\lambda + 2\mu)\, \epsilon_o e^{i\omega t} \quad . \end{aligned} \tag{b}$$

Finally, a set of surface tractions which are equal and opposite to those of Eq. (b) are applied to the cylinder (Fig. III-1c).

The superposition of the three states of stress of Fig. (III-1) shows that the pressure field which is produced in the fluid by the uniform straining of the cylinder, $\epsilon_{zz} = \epsilon_o e^{i\omega t}$, is equivalent to that which is produced by the fictitious surface tractions of Fig. (III-1c), namely

$$\begin{aligned} \sigma_{rr} &= \lambda \epsilon_o e^{i\omega t} \\ \sigma_{zz} &= (\lambda + 2\mu)\, \epsilon_o e^{i\omega t} \quad . \end{aligned} \tag{c}$$

For the illustrative problem, the parameters $\nu = \frac{1}{4}$ and $\lambda\varepsilon_o = 10^3 \ \frac{lb}{in^2}$ have been chosen. The problem thus consists of the evaluation of the pressure field produced in the fluid by the fictitious time harmonic tractions $\sigma_{rr} = 10^3 \ e^{i\omega t}$ and $\sigma_{zz} = 3(10^3) \ e^{i\omega t}$ which are applied on the boundary surfaces of the elastic cylinder.

The following parameters are used in the numerical example:

1. Elastic Cylinder

   $L = 2a$

   $\nu = \frac{1}{4}$ (i.e. $\lambda = \mu$)

   $\mu = 12(10^6)$ lb/in^3

   $w = 0.2833$ lb/in^3

2. Acoustic Fluid

   $w_f = 62.5$ lb/ft^3

   $c_3 = 5000$ ft/sec

3. Computational Geometry and Pressure Loading [See Fig. III-2].

   [6 side bands on the surface $r = a$
   6 ring bands on the surface $z = 0$
   6 ring bands on the surface $z = L$]. } $N = 18$ bands.

4. Symmetrical Loading: $P_{rr,oj} = (10^3) \ e^{i\omega t}$ j on the surface $r = a$

   $P_{zz,oj} = 3(10^3) \ e^{i\omega t}$ j on surfaces $z = 0$ and $z = L$

With the input values chosen, the propagation velocities of the pressure and shear waves in the medium become respectively

$$c_1 = \frac{\lambda + 2\mu}{\rho} = \frac{3\mu g}{w} = 18{,}460 \text{ ft/sec.}$$

$$c_2 = \frac{\mu}{\rho} = \frac{\mu g}{w} = 10{,}660 \text{ ft/sec.}$$

$$c_3 \text{ (fluid)} = 5{,}000 \text{ ft/sec.}$$

The following values of the nondimensional parameters $\bar{k}_n = \frac{\omega a}{c_n}$ were used in the computations:

$$\bar{k}_1 = 0.5444$$
$$\bar{k}_2 = 0.9425$$
$$\bar{k}_3 = 2.0100$$

For example, a possible combination of forcing frequency ω and cylinder radius for which the numerical results would apply is $\omega = 400$ cps and $a = 4$ ft.

The cylinder geometry for the choice of $N = 18$ bands is shown in Fig. (III-2). It should be emphasized that this value of N was chosen only as a reasonable computational geometry to illustrate the general method in a sensible manner. It does not necessarily represent, however, the number of bands which might be required to obtain physically meaningful results of sufficient accuracy for application to practical problems. In the latter case, a larger number of bands N would generally be required.

a) Computation of the Real and Imaginary Portions of the Coefficients α_{oji} , β_{oji} , γ_{oji} and their Space Derivatives.

Some representative numerical values of the coefficients $\bar{\alpha}_{oji}$, $\bar{\bar{\alpha}}_{oji}$, their space derivatives, and the corresponding quantities for β_{oji} and γ_{oji} are given in this section for the illustrative problem. Recalling that each coefficient is written in terms of a real and imaginary part e.g.

$$\alpha_{oji} = \bar{\alpha}_{oji} + i\,\bar{\bar{\alpha}}_{oji} \quad ,$$

analytical expressions for these quantities are given in Appendix B and Appendix C of Reference [1].

For the cases in which $i \neq j$, the quantities $\bar{\alpha}_{oji}$, $\bar{\beta}_{oji}$, $\bar{\gamma}_{oji}$ and their space derivatives are evaluated by numerical integration [Simpson's Rule], using Eqs. (B-7)-(B-15) of Reference [1]. Sharp peaks which occur in the integrands for values of $\psi < 40^{\circ}$ necessitated the use of a variable spacing in the numerical integration as follows:

ψ(degrees)	$\Delta\psi$(degrees)
0 - 8	1
8 - 20	3
20 - 40	5
40 - 60	10
60 - 180	20

A similar numerical integration was used to evaluate the quantities $\bar{\bar{\alpha}}_{oji}$, $\bar{\bar{\beta}}_{oji}$, $\bar{\bar{\gamma}}_{oji}$ and their derivatives, Eqs. (B-16)-(B-24) of Reference [1]. For each quantity, an integration spacing of $\Delta\psi = 18$ degrees was used.

For small values of the variable X, computational accuracy required that certain of the trigonometric expressions appearing in these equations be expanded into power series so that the leading terms in the integrand could be cancelled analytically. Expressions for the evaluation of these coefficients are obtained by setting n = 0 in Eqs. (A-27)-(A-35) of this paper. Equations (A-36)-(A-38) give the analytical expressions and the range of application for the functions appearing in the integrands. It should be noted that these ranges will vary for different problems and that they must be determined separately in each case by a series of trial integrations using the expressions given in Eqs. (A-36)-(A-38).

For the case i = j in which the field points and the source points are on the same band special formulas are required for the evaluation of the coefficients $\bar{\alpha}_{oji}$, $\bar{\beta}_{oji}$, $\bar{\gamma}_{oji}$ and their derivatives because of an infinite discontinuity in their integrands at the value defined by R = 0. To evaluate these improper (but convergent) integrals, Eqs. (126)-(127) and Eqs. (C-4)-(C-8) of Reference [1] are used. The values of the limit $\bar{\theta}$ in Eqs. (126)-(127) are evaluated separately by trial integrations in each case.

Table II gives the nondimensional values of the quantities ρ, $\bar{\rho}$ and $(\xi-\bar{\xi})$ for the calculation of the real and imaginary parts of the coefficients α_{oji} , β_{oji} and γ_{oji} and their derivatives in the illustrative problem. While it is not practical to list the values of these coefficients for all combinations of i and j, some representative values of these quantities for the two cases j = 7, i = 6 and j = 3, i = 9 are given in Table III for the convenience of those readers who may wish to work through a sample computation. Representative values for the evaluation of the real portions of the coefficients α_{oii} and its pertinent derivatives are given in Table IV for the two cases, i = j = 5 (top band) and i = j = 7 (side band).

Table II - Nondimensional Values of the ρ, $\bar{\rho}$ and $(\xi-\bar{\xi})$ - Illustrative Problem

	i =	1	2	3	4	5	6	7	8	9	10	11	12	13	14	15	16	17	18
	$\bar{\rho}$ =	$\frac{1}{12}$	$\frac{1}{4}$	$\frac{5}{12}$	$\frac{7}{12}$	$\frac{3}{4}$	$\frac{11}{12}$	1	1	1	1	1	1	$\frac{11}{12}$	$\frac{3}{4}$	$\frac{7}{12}$	$\frac{5}{12}$	$\frac{1}{4}$	$\frac{1}{12}$
J	ρ	$(\xi-\bar{\xi})$ →																	
1	$\frac{1}{12}$	0	0	0	0	0	0	$\frac{1}{6}$	$\frac{1}{2}$	$\frac{5}{6}$	$\frac{7}{6}$	$\frac{3}{2}$	$\frac{11}{6}$	2	2	2	2	2	2
2	$\frac{1}{4}$	0	0	0	0	0	0	$\frac{1}{6}$	$\frac{1}{2}$	$\frac{5}{6}$	$\frac{7}{6}$	$\frac{3}{2}$	$\frac{11}{6}$	2	2	2	2	2	2
3	$\frac{5}{12}$	0	0	0	0	0	0	$\frac{1}{6}$	$\frac{1}{2}$	$\frac{5}{6}$	$\frac{7}{6}$	$\frac{3}{2}$	$\frac{11}{6}$	2	2	2	2	2	2
4	$\frac{7}{12}$	0	0	0	0	0	0	$\frac{1}{6}$	$\frac{1}{2}$	$\frac{5}{6}$	$\frac{7}{6}$	$\frac{3}{2}$	$\frac{11}{6}$	2	2	2	2	2	2
5	$\frac{3}{4}$	0	0	0	0	0	0	$\frac{1}{6}$	$\frac{1}{2}$	$\frac{5}{6}$	$\frac{7}{6}$	$\frac{3}{2}$	$\frac{11}{6}$	2	2	2	2	2	2
6	$\frac{11}{12}$	0	0	0	0	0	0	$\frac{1}{6}$	$\frac{1}{2}$	$\frac{5}{6}$	$\frac{7}{6}$	$\frac{3}{2}$	$\frac{11}{6}$	2	2	2	2	2	2
7	1	$-\frac{1}{6}$	$-\frac{1}{6}$	$-\frac{1}{6}$	$-\frac{1}{6}$	$-\frac{1}{6}$	$-\frac{1}{6}$	0	$\frac{1}{3}$	$\frac{2}{3}$	1	$\frac{4}{3}$	$\frac{5}{3}$	$\frac{11}{6}$	$\frac{11}{6}$	$\frac{11}{6}$	$\frac{11}{6}$	$\frac{11}{6}$	$\frac{11}{6}$
8	1	$-\frac{1}{2}$	$-\frac{1}{2}$	$-\frac{1}{2}$	$-\frac{1}{2}$	$-\frac{1}{2}$	$-\frac{1}{2}$	$-\frac{1}{3}$	0	$\frac{1}{3}$	$\frac{2}{3}$	1	$\frac{4}{3}$	$\frac{3}{2}$	$\frac{3}{2}$	$\frac{3}{2}$	$\frac{3}{2}$	$\frac{3}{2}$	$\frac{3}{2}$
9	1	$-\frac{5}{6}$	$-\frac{5}{6}$	$-\frac{5}{6}$	$-\frac{5}{6}$	$-\frac{5}{6}$	$-\frac{5}{6}$	$-\frac{2}{3}$	$-\frac{1}{3}$	0	$\frac{1}{3}$	$\frac{2}{3}$	1	$\frac{7}{6}$	$\frac{7}{6}$	$\frac{7}{6}$	$\frac{7}{6}$	$\frac{7}{6}$	$\frac{7}{6}$

Table III - Representative Values of α_{oji} , β_{oji} , γ_{oji} and their Space Derivatives - i = j

		CASE I		CASE II	
		J = 7, i = 6		J = 3, i = 9	
κ_i		Real Portion (single bar)	Imaginary Portion (double bar)	Real Portion (single bar)	Imaginary Portion (double bar)
$\kappa_1 = .5444$	α_{oji}	-.4858500	+.2274170	-.2860010	+.2478359
	α^{z}_{oji}	-.7521002	+.003887410	+.2421691	-.02119497
	α^{r}_{oji}	+.6153040	-.02273441	+.03017070	-.01027833
	α^{rz}_{oji}	+ 3.910194	-.0002299027	+.04672336	+.0005205666
	α^{rzz}_{oji}	+ 47.68267	+.001377773	-.2926517	+.0006060587
	α^{zrr}_{oji}	+ 4.430315	-.0002201813	----	----
	α^{zz}_{oji}	----	----	-.09011387	-.02437010
	α^{rr}_{oji}	+ 2.074596	-.02138003	----	----
	α^{zzz}_{oji}	----	----	-.2010604	+.003792008
$\kappa_2 = .9425$	β_{oji}	-.3542777	+.3262738	-.1225355	+.3522680
	β^{z}_{oji}	-.7726809	+.01807612	+.2918503	-.09819865
	β^{r}_{oji}	+.6556329	-.09997833	+.03667484	-.04451797
	β^{rz}_{oji}	+ 3.941736	-.003183777	+.03799412	+.007139976
	β^{rzz}_{oji}	+ 47.68707	+.01903262	-.3136065	+.007779862
	β^{zrr}_{oji}	+ 4.533949	-.002781721	----	----
	β^{zz}_{oji}	----	----	-.09717981	-.1025629
	β^{rr}_{oji}	+ 2.119123	-.08195736	----	----
	β^{zzz}_{oji}	----	----	-.3392487	+.05333224
$\kappa_3 = 2.01$	γ_{oji}	-.06006077	+.2492022	+.3011386	+.1673313
	γ^{z}_{oji}	-.8155342	+.1005983	+.1056342	-.4913962
	γ^{r}_{oji}	+.4507052	-.3588395	-.1396592	-.1167767

Table IV - Representative Values of α_{oii} and its Space Derivatives — i = j

	i = j = 5	i = j = 7
	$\frac{\bar{a}}{a}$ = .1180	$\frac{\bar{a}}{a}$ = .1750
	λa = 6.00	λa = 2.97
$\bar{\alpha}$	-.6800	-.63758
$\bar{s}_\alpha$	-.3540	-.2590
$a\bar{\alpha}^z$	+ 3.00	0
$a\bar{s}_\alpha^z$	+ 3.00	0
$a\bar{\alpha}^r$	+.34636	+ 1.8215
$a\bar{s}_\alpha^r$	0	+ 1.4850
$a^2\bar{\alpha}^{rz}$	0	0
$a^2\bar{s}_\alpha^{rz}$	0	0
$a^3\bar{\alpha}^{rzz}$	+ 59.820	+ 11.401
$a^3\bar{s}_\alpha^{rzz}$	0	0
$a^2\bar{\alpha}^{zz}$	- 20.582	---
$a^2\bar{s}_\alpha^{zz}$	- 25.404	---
$a^3\bar{\alpha}^{zzr}$	-.88911	---
$a^3\bar{s}_\alpha^{zzz}$	-.88911	---
$a^3\bar{\alpha}^{zrr}$	---	0
$a^3\bar{s}_\alpha^{zrr}$	---	0
$a^2\bar{\alpha}^{rr}$	---	- 5.4126
$a^2\bar{s}_\alpha^{rr}$	---	- 8.50

b) Determination of the Set of Simultaneous Linear Equations on the Source Strengths G_{oi} , H_{oi} and C_{oi} .

As for the case n ≠ 0, the source strengths and the coefficients α_{oji} , β_{oji} , γ_{oji} and their space derivatives are written in terms of their real and imaginary parts, e.g.

$$G_{oi} = \bar{G}_{oi} + i\,\bar{\bar{G}}_{oi}$$

$$\alpha_{oi} = \bar{\alpha}_{oi} + i\,\bar{\bar{\alpha}}_{oi}$$

and the real and imaginary parts of Eqs. (117)-(122) are equated, thus leading to the following set of equations in computational form:

Point j on the surface r = a

$$\mathrm{Re}\,\sigma_{rr} = \sum_{i=1}^{N}\left\{\bar{G}_{oi}\bar{d}_1 - \bar{\bar{G}}_{oi}\bar{\bar{d}}_1 + \bar{H}_{oi}a\bar{d}_2 - \bar{\bar{H}}_{oi}a\bar{\bar{d}}_2 + \bar{C}_{oi}\bar{d}_4 + \bar{\bar{C}}_{oi}\bar{\bar{d}}_4\right\}_{r=a} = P_{rr,oj} \qquad \text{(III-1)}$$

$$\mathrm{Im}\,\sigma_{rr} = \sum_{i=1}^{N}\left\{\bar{G}_{oi}\bar{\bar{d}}_1 + \bar{\bar{G}}_{oi}\bar{d}_1 + \bar{H}_{oi}a\bar{\bar{d}}_2 + \bar{\bar{H}}_{oi}a\bar{d}_2 - \bar{C}_{oi}\bar{\bar{d}}_4 + \bar{\bar{C}}_{oi}\bar{d}_4\right\}_{r=a} = 0 \qquad \text{(III-2)}$$

$$\mathrm{Re}\,\sigma_{rz} = \sum_{i=1}^{N}\left\{\bar{G}_{oi}\bar{d}_5 - \bar{\bar{G}}_{oi}\bar{\bar{d}}_5 + \bar{H}_{oi}a\bar{d}_6 - \bar{\bar{H}}_{oi}a\bar{\bar{d}}_6\right\}_{r=a} = 0 \qquad \text{(III-3)}$$

$$\mathrm{Im}\,\sigma_{rz} = \sum_{i=1}^{N}\left\{\bar{G}_{oi}\bar{\bar{d}}_5 + \bar{\bar{G}}_{oi}\bar{d}_5 + \bar{H}_{oi}a\bar{\bar{d}}_6 + \bar{\bar{H}}_{oi}a\bar{d}_6\right\}_{r=a} = 0 \qquad \text{(III-4)}$$

$$\mathrm{Re}\,\dot{w} = \sum_{i=1}^{N}\left\{-\bar{G}_{oi}\bar{\bar{\alpha}}^{r}_{oji} - \bar{\bar{G}}_{oi}\alpha^{r}_{oji} + \bar{H}_{oi}a\bar{\bar{\beta}}^{rz}_{oji} + \bar{\bar{H}}_{oi}a\beta^{rz}_{oji} + \frac{\bar{C}_{oi}}{\omega}\gamma^{r}_{oji} - \frac{\bar{\bar{C}}_{oi}}{\omega}\bar{\bar{\gamma}}^{r}_{oji}\right\}_{r=a} = 0$$

(III-5)

$$\text{Im } \dot{v} = \sum_{i=1}^{N} \left\{ \tilde{G}_{oi} \bar{\alpha}^{r}_{oji} - \bar{\tilde{G}}_{oi} \bar{\tilde{\alpha}}^{r}_{oji} - \tilde{H}_{oi} a\bar{\beta}^{rz}_{oji} + \bar{\tilde{H}}_{oi} a\bar{\tilde{\beta}}^{rz}_{oji} + \frac{\tilde{C}_{oi}}{\omega} \bar{\gamma}^{r}_{oji} + \frac{\bar{\tilde{C}}_{oi}}{\omega} \bar{\tilde{\gamma}}^{r}_{oji} \right\}_{r=a} = 0 \quad .$$

(III-6)

Point j on end surfaces, z = 0 and z = L.

$$\text{Re } \sigma_{zz} = \sum_{i=1}^{N} \left\{ \tilde{G}_{oi} \tilde{d}_{11} - \bar{\tilde{G}}_{oi} \bar{\tilde{d}}_{11} + \tilde{H}_{oi} a\tilde{d}_{12} - \bar{\tilde{H}}_{oi} a\bar{\tilde{d}}_{12} + \tilde{C}_{oi} \tilde{d}_{4} + \bar{\tilde{C}}_{oi} \bar{\tilde{d}}_{4} \right\}_{z=0,L} = P_{zz,oj}$$

(III-7)

$$\text{Im } \sigma_{zz} = \sum_{i=1}^{N} \left\{ \tilde{G}_{oi} \bar{\tilde{d}}_{11} + \bar{\tilde{G}}_{oi} \tilde{d}_{11} + \tilde{H}_{oi} a\bar{\tilde{d}}_{12} + \bar{\tilde{H}}_{oi} a\tilde{d}_{12} - \tilde{C}_{oi} \bar{\tilde{d}}_{4} + \bar{\tilde{C}}_{oi} \tilde{d}_{4} \right\}_{z=0,L} = 0 \quad \text{(III-8)}$$

$\text{Re } \sigma_{rz} = 0$ Apply Eq. (III-3) at point.

$\text{Im } \sigma_{rz} = 0$ Apply Eq. (III-4) at point.

$$\text{Re } \dot{u} = \sum_{i=1}^{N} \left\{ - \tilde{G}_{oi} \bar{\tilde{\alpha}}^{z}_{oji} - \bar{\tilde{G}}_{oi} \bar{\alpha}^{z}_{oji} + \tilde{H}_{oi} \bar{\tilde{d}}_{15} + \bar{\tilde{H}}_{oi} \tilde{d}_{15} + \frac{\tilde{C}_{oi}}{\omega} \bar{\gamma}^{z}_{oji} - \frac{\bar{\tilde{C}}_{oi}}{\omega} \bar{\tilde{\gamma}}^{z}_{oji} \right\}_{z=0,L} = 0$$

(III-9)

$$\text{Im } \dot{u} = \sum_{i=1}^{N} \left\{ \tilde{G}_{oi} \bar{\alpha}^{z}_{oji} - \bar{\tilde{G}}_{oi} \bar{\tilde{\alpha}}^{z}_{oji} - \tilde{H}_{oi} a\bar{\tilde{d}}_{15} + \bar{\tilde{H}}_{oi} a\tilde{d}_{15} + \frac{\tilde{C}_{oi}}{\omega} \bar{\tilde{\gamma}}^{z}_{oji} + \frac{\bar{\tilde{C}}_{oi}}{\omega} \bar{\gamma}^{z}_{oji} \right\}_{z=0,L} = 0 \quad .$$

(III-10)

Expressions for the coefficients $\tilde{d}_k$ and $\bar{\tilde{d}}_k$ are obtained by setting n = 0 in the expressions which are given in Table I of this report [See Pg. 15].

For the illustrative problem under consideration, a symmetrical fictitious pressure loading about the plane $z = \frac{L}{2}$ of the cylinder is applied. Consequently, for $N = 18$ bands, the system of $6N$ equations reduces to one of $3N = 54$ equations on the real and imaginary portions of the source strengths.

A convenient form which illustrates the order of the matrix coefficients for the source strength equations, which was used in the present problem is given in Table V. The rows of the matrix, denoted by p, represent the expressions for the real and imaginary portions of the stresses and velocities at each of the indicated field points j, while the columns, denoted by q, indicate the coefficients of the appropriate source strengths at each of the indicated source points i. The last column represents the forcing function which is applied to the cylinder. It should be noted that the symbols $\bar{d}_k^*$ which appear in Table VI are defined in terms of the $\bar{d}_k$ coefficients of Table I as follow:

$$\bar{d}_k^* = \frac{a^2}{2\mu}\left[\bar{d}_{oj1k} + \bar{d}_{oj(19-1)k}\right] . \qquad \text{(III-11)}$$

While it is not practical to list all of the numerical values of the matrix coefficients for the illustrative problem being considered, some representative values of these quantities for the cases $q = 1$ to 4 and $p = 1$ to 20 are given in Table VI for the convenience of those readers who may wish to work through a sample computation.

c) Solution of the Set of Simultaneous Linear Equations on the Source Strengths C_{oi} , H_{oi} and C_{oi} .

The solution of the system of the 54 linear simultaneous equations on the real and imaginary parts of the source strength coefficients can be approached in two ways. First, the homogeneous equations in the system can be used to eliminate a number of the unknowns such that the 6N system reduces to a series of 2N systems which may then be solved on an electronic computer. This procedure would be justified in a large problem in which a system of several hundred equations would have to be solved. For the present problem, however, it is a comparatively simple matter to solve the system of 54 equations directly, using an IBM 7090 computer. The values of the source strength coefficients are given in Table VII.

Table V - Illustrative Problem - Matrix Coefficients of Source Strength Equations n = 0

	Matrix q Column	q = 1-9	10-18	19-27	28-36	37-45	46-54	55
	Source Point Index = i	i = 1-9	1-9	1-9	1-9	1-9	1-9	
Matrix p Row	Field Point Index = j		$\bar{G}_{oi}$	$\bar{\bar{G}}_{oi}$	$\bar{H}_{oi}$	$\bar{\bar{H}}_{oi}$	$\bar{C}_{oi}$	C_{oi}	$P_{nn,oj}$
p = 1 to 6	j = 1-6	Re σ_{zz}	$\bar{d}^{*}_{11}$	$-\bar{\bar{d}}^{*}_{11}$	$a\bar{d}^{*}_{12}$	$-a\bar{\bar{d}}^{*}_{12}$	$\bar{d}^{*}_{4}$	$\bar{d}^{*}_{4}$	$\frac{a^2}{2\mu} P_{zz,oj}$
7-9	7-9	Re σ_{rr}	$\bar{d}^{*}_{1}$	$-\bar{\bar{d}}^{*}_{1}$	$a\bar{d}^{*}_{2}$	$-a\bar{\bar{d}}^{*}_{2}$	$\bar{d}^{*}_{4}$	$\bar{d}^{*}_{4}$	$\frac{a^2}{2\mu} P_{rr,oj}$
10-15	1-6	Im σ_{zz}	$\bar{\bar{d}}^{*}_{11}$	$\bar{d}^{*}_{11}$	$a\bar{\bar{d}}^{*}_{12}$	$a\bar{d}^{*}_{12}$	$-\bar{d}^{*}_{4}$	$\bar{\bar{d}}^{*}_{4}$	0
16-18	7-9	Im σ_{rr}	$\bar{\bar{d}}^{*}_{1}$	$\bar{d}^{*}_{1}$	$a\bar{\bar{d}}^{*}_{2}$	$a\bar{d}^{*}_{2}$	$\bar{d}^{*}_{4}$	$-\bar{\bar{d}}^{*}_{4}$	0
19-27	1-9	Re σ_{rz}	$\bar{d}^{*}_{5}$	$-\bar{\bar{d}}^{*}_{5}$	$a\bar{d}^{*}_{6}$	$-a\bar{\bar{d}}^{*}_{6}$	0	0	0
28-36	1-9	Im σ_{rz}	$\bar{\bar{d}}^{*}_{5}$	$\bar{d}^{*}_{5}$	$a\bar{\bar{d}}^{*}_{6}$	$a\bar{d}^{*}_{6}$	0	0	0
37-42	1-6	Re $\dot{u}$	$-a\bar{\bar{\alpha}}^{z}_{oji}$	$-a\bar{\alpha}^{z}_{oji}$	$\frac{2\mu}{a}\bar{\bar{d}}^{*}_{16}$	$\frac{2\mu}{a}\bar{d}^{*}_{16}$	$\frac{a}{\omega}\bar{\gamma}^{z}_{oji}$	$-\frac{a}{\omega}\bar{\bar{\gamma}}^{z}_{oji}$	0
43-45	7-9	Re $\dot{w}$	$-a\bar{\bar{\alpha}}^{r}_{oji}$	$-a\bar{\alpha}^{r}_{oji}$	$a^2\bar{\beta}^{rz}_{oji}$	$a^2\bar{\bar{\beta}}^{rz}_{oji}$	$\frac{a}{\omega}\bar{\gamma}^{r}_{oji}$	$-\frac{a}{\omega}\bar{\bar{\gamma}}^{r}_{oji}$	0
46-51	1-6	Im $\dot{u}$	$a\bar{\alpha}^{z}_{oji}$	$-a\bar{\bar{\alpha}}^{z}_{oji}$	$-a^2\bar{d}^{*}_{16}$	$a^2\bar{\bar{d}}^{*}_{16}$	$\frac{a}{\omega}\bar{\bar{\gamma}}^{z}_{oji}$	$\frac{a}{\omega}\bar{\gamma}^{z}_{oji}$	0
52-54	7-9	Im $\dot{w}$	$a\bar{\alpha}^{r}_{oji}$	$-a\bar{\bar{\alpha}}^{r}_{oji}$	$-a^2\bar{\beta}^{rz}_{oji}$	$a^2\bar{\bar{\beta}}^{rz}_{oji}$	$\frac{a}{\omega}\bar{\bar{\gamma}}^{r}_{oji}$	$\frac{a}{\omega}\bar{\gamma}^{r}_{oji}$	0

NOTE: $\bar{d}^{*}_{k} = \frac{a^2}{2\mu}\left[\bar{d}_{ojik} + \bar{d}_{oj(19-i)k}\right]$. See Table (1) and Footnote (6) .

Table VI - Numerical Values of Matrix Coefficients q = 1 to 4; p = 1 to 20.

p \ q	1	2	3	4
1	- 19.108	+ 10.552	+ 3.2568	+ 1.6250
2	+ 3.5100	+ 22.599	+ 7.7992	+ 2.4019
3	+.65136	+ 4.6795	- 23.672	+ 7.0535
4	+.23214	+ 1.0294	+ 5.0086	- 20.832
5	+.11003	+.41256	+ 1.1664	+ 5.2229
6	+.061533	+.21305	+.48891	+ 1.2406
7	-.068969	-.22186	-.42763	-.74187
8	-.032897	-.091414	-.11941	-.063712
9	-.0085599	-.016324	+.0035093	+.070570
10	-.0098308	-.029421	-.048797	-.067817
11	-.0098062	-.029349	-.048678	-.067653
12	-.0097593	-.029207	-.048443	-.067326
13	-.0096882	-.028994	-.048090	-.066837
14	-.0095939	-.028712	-.047623	-.066189
15	-.0095101	-.028362	-.047043	-.065384
16	-.0097595	-.029190	-.048358	-.067078
17	-.0099396	-.029730	-.049253	-.068334
18	-.010031	-.030002	-.049705	-.068963
19	-.0016023	-.0045155	-.0066488	-.0077498
20	-.0046601	-.013163	-.020737	-.026749

Table VII - Source Strength Coefficients.

Source Point i	$\bar{C}_{oi}$	$\bar{\bar{C}}_{oi}$	$(10^2)\ \bar{G}_{oi}$	$(10^2)\ \bar{\bar{G}}_{oi}$	$(10^3)\ \bar{H}_{oi}$	$(10^3)\ \bar{\bar{H}}_{oi}$
i = 1	- 17.411	37.887	- 1.7202	+ .16903	+ .0040134	+ .00011319
2	- 16.741	31.727	- 1.3930	+ .13424	- .043571	+ .0012951
3	- 14.030	24.860	- 1.2899	+ .11856	+ .12250	+ .0039739
4	- 9.4095	38.316	- 1.3449	+ .11274	- .27677	+ .0089387
5	- 2.9858	17.601	- 1.2055	+ .082023	+ .43680	+ .019710
6	8.2628	36.282	- .74770	+ .028792	- .81265	+ .048730
7	- 45.238	7.0447	- .65266	+ .26290	- .93899	- .13509
8	- 47.408	24.673	- 1.0528	+ .39733	- .78204	- .051806
9	- 50.463	28.362	- 1.2582	+ .43650	- .088151	- .025014

d) Evaluation of the Fluid Pressure Field.

The complex pressure and velocity components at field points in the fluid are evaluated from the relations

$$p_{o,j} = \sum_{i=1}^{N} \rho_f \omega e^{i\omega t} \left[- \left(\bar{\bar{C}}_{oi} \bar{\gamma}_{oji} + \bar{C}_{oi} \bar{\bar{\gamma}}_{oji} \right) + i \left(\bar{C}_{oi} \bar{\gamma}_{oji} - \bar{\bar{C}}_{oi} \bar{\bar{\gamma}}_{oji} \right) \right] \qquad \text{(III-12)}$$

$$v_{o,j} = \sum_{i=1}^{N} e^{i\omega t} \left[- \left(\bar{C}_{oi} \bar{\gamma}^{r}_{oji} - \bar{\bar{C}}_{oi} \bar{\bar{\gamma}}^{r}_{oji} \right) - i \left(\bar{C}_{oi} \bar{\bar{\gamma}}^{r}_{oji} + \bar{\bar{C}}_{oi} \bar{\gamma}^{r}_{oji} \right) \right] \qquad \text{(III-13)}$$

$$v_{o,j} = \sum_{i=1}^{N} e^{i\omega t} \left[- \left(\bar{C}_{oi} \bar{\gamma}^{z}_{oji} - \bar{\bar{C}}_{oi} \bar{\bar{\gamma}}^{z}_{oji} \right) - i \left(\bar{C}_{oi} \bar{\bar{\gamma}}^{z}_{oji} + \bar{\bar{C}}_{oi} \bar{\gamma}^{z}_{oji} \right) \right] \qquad \text{(III-14)}$$

The coefficients $\bar{\gamma}_{oji}$, $\bar{\bar{\gamma}}_{oji}$ and their space derivatives are evaluated from Eqs. (A-1)-(A-38) of Appendix A of this paper where R is the distance between the source point i and the field point j in the acoustic fluid at which the pressure and/or velocities are being computed.

The quantity $X = \frac{k_3 R}{a}$ is given by Eq. (A-4) where $\rho = \frac{R_o}{a} \cos \bar{\zeta}$; $\xi = \frac{R_o}{a} \sin \bar{\zeta}$, and R_o represents the distance from the field point j at which the pressure is being evaluated, to a reference point O which for convenience is located at the center of the cylinder, i.e. at the point O defined by the coordinates r = 0 and z = $\frac{L}{2}$, Fig (III-3).

The far field pressures in the fluid, i.e. the pressures at distances R which are large multiples of the cylinder dimensions, are of practical interest. A simplified asymptotic expression for the fluid pressure, $p_{o,j}$ in the far field, was derived in Reference [1] in terms of the fluid source strength coefficients C_{oi} and a prescribed distance and slope angle, R_o and ζ respectively, as shown in Fig. (III-3). For the axisymmetrical loading and geometry of the present

problem, the asymptotic value of the far field fluid pressure is given by the relation

$$p_{o,j} = \left[-\frac{i\rho_f \omega}{2} \sum_{i=1}^{N} C_{oi} \bar{r}\, e^{ik_3 \bar{z} \sin \bar{\xi}}\, J_o(k_3 \bar{r} \cos \bar{\xi})\, e^{i\omega t} \right] \frac{e^{-\frac{i\omega R_o}{c}}}{R_o} \quad . \qquad \text{(III-15)}$$

It should be noted that once the pressure $p_{o,j}$ has been evaluated from Eq. (III-15) for a given point P_j on the ray specified by R_o and $\bar{\xi}$, it can easily be evaluated for any other point on the ray by changing the scale factor

$$\frac{e^{-\frac{i\omega R_o}{c}}}{R_o} \quad ,$$

since the quantity in the bracket will be a constant for a given ray. The use of Eq. (III-15) in the evaluation of the far field fluid pressure greatly simplifies the computation which would be required if Eq. (III-12) were to be used, since it eliminates the necessity for the numerical computation of the γ_{oj1} integral coefficients for each field point j in the fluid.

A simple formula for the evaluation of the absolute value of the pressure $p_{o,j}$ in the far field is given by the relation

$$p_{o,j} \doteq \frac{\rho_f \omega}{2} \left| \sum_{i=1}^{N} C_{oi} \bar{r}\, \frac{e^{ik_3 \bar{z} \sin \bar{\xi}}}{R_c}\, J_o(k_3 \bar{r} \cos \bar{\xi}) \right| \frac{R_c}{R_o} \doteq \frac{C_{Ray}}{\left[\frac{R_o}{R_c}\right]} \qquad \text{(III-16)}$$

where R_c refers to some reference point on the ray under consideration and R_o refers to the field point on the ray at which the pressure is to be evaluated. For points which are closer to the cylinder so that the asymptotic formula for the fluid pressure cannot be used, the absolute value of the pressure $p_{o,j}$ is given by the relation,

$$p_{o,j} = \rho_f \omega \left\{ \left[\sum_{i=1}^{N} \left(\bar{\bar{C}}_{oi} \bar{\bar{\gamma}}_{oji} + \bar{\bar{\bar{C}}}_{oi} \bar{\bar{\gamma}}_{oji} \right) \right]^2 + \left[\sum_{i=1}^{N} \left(\bar{\bar{C}}_{oi} \bar{\bar{\gamma}}_{oji} - \bar{\bar{\bar{C}}}_{oi} \bar{\bar{\gamma}}_{oji} \right) \right]^2 \right\}^{\frac{1}{2}} \qquad \text{(III-17)}$$

Numerical computations for the absolute value of the pressure $p_{o,j}$ have been carried out along rays ranging from $0^\circ(22\frac{1}{2}^\circ)90^\circ$ as shown in Figs. (III-4) and (III-5). In each figure, the lines of constant pressure in the fluid are shown. The results which are plotted have all been derived using Eq. (III-17) and checked, beyond $R_o = 20a$, by Eq. (III-16). For the benefit of those who may wish to work through a sample computation, a representative set of numerical values is given in Table VIII. The values of the constants C_{Ray} appearing in Eq. (III-16) are given in Table IX. In the present example, Eq. (III-16) can be used with good accuracy for those points for which $R_o > 20a$.

It must once again be emphasized that these numerical results may not represent an accurate solution of this problem because too few bands were purposely used in the computational work for the cylinder and fluid source strength coefficients. This was done in order to present the simplest possible numerical example which illustrated all the complexities of the application of the general method. For a practical problem with a real transducer, a considerably finer finite difference breakup would be required in order to evaluate accurate values of the pressures in the fluid.

Table VIII - Computation for Pressure in Fluid - Numerical Example;

Ray 3, $\bar{i} = 45^\circ$, $\frac{R_o}{a} = 7.07$.

i	$\tilde{\rho}$	$\bar{i}$	$\bar{\gamma}_{oji}$	$\bar{\bar{\gamma}}_{oji}$
1	$\frac{1}{12}$	1	- .006182	+ .0019395
2	$\frac{1}{4}$	1	- .017912	+ .0056330
3	$\frac{5}{12}$	1	- .027798	+ .0087756
4	$\frac{7}{12}$	1	- .034809	+ .011021
5	$\frac{3}{4}$	1	- .038191	+ .012058
6	$\frac{11}{12}$	1	- .037537	+ .011626
7	1	$\frac{5}{6}$	- .032898	+ .018512
8	1	$\frac{1}{2}$	- .022015	+ .031663
9	1	$\frac{1}{6}$	- .0054818	+ .038822
10	1	$-\frac{1}{6}$	+ .013308	+ .037387
11	1	$-\frac{1}{2}$	+ .029733	+ .026771
12	1	$-\frac{5}{6}$	+ .03918	+ .0089625
13	$\frac{11}{12}$	- 1	+ .040008	- .0011364
14	$\frac{3}{4}$	- 1	+ .037455	- .00062594
15	$\frac{7}{12}$	- 1	+ .032249	- .00022219
16	$\frac{5}{12}$	- 1	+ .024782	+ .000022490
17	$\frac{1}{4}$	- 1	+ .015590	+ .000097948
18	$\frac{1}{12}$	- 1	+ .0053192	+ .000047970

$p_{o,j} = + .001860 - .0014081$; $|p_{o,j}| = .002333$ psi.

Table IX - C_{Ray} Values [$R_c = 20a$].

ξ	C_{Ray} [Eq. III-16]	C_{Ray} [Calculated from Eq. (III-17) at R = 20a]
0°	0.9204	0.910
22.5°	0.8929	0.883
45°	0.8168	0.824
67.5°	0.7559	0.788
90°	0.7456	0.798

IV DISCUSSION AND CONCLUSIONS.

This paper is part of a study on the development of methods for treating the forced vibrations of elastic bodies of revolution submerged in an acoustic fluid. A method, based on a potential theory approach, for the evaluation of the pressure field in an infinite acoustic fluid due to the harmonic excitation of an elastic circular cylindrical body of finite length has been derived in Reference [1] and is illustrated in the present paper.

The illustrative example is presented for the case of an axisymmetrical (θ independent) excitation of the cylinder. The application of the method to more general excitations of the cylindrical body, which vary in both z and θ, follow a similar computational pattern and are described in Part II of this report.

The general procedures may find application in problems relating to the response of fluid to the harmonic excitation of large cylindrical transducers. In addition, the general approach is also being applied to problems involving the evaluation of fluid pressures produced by the harmonic excitations of submerged cylindrical shells of finite length.

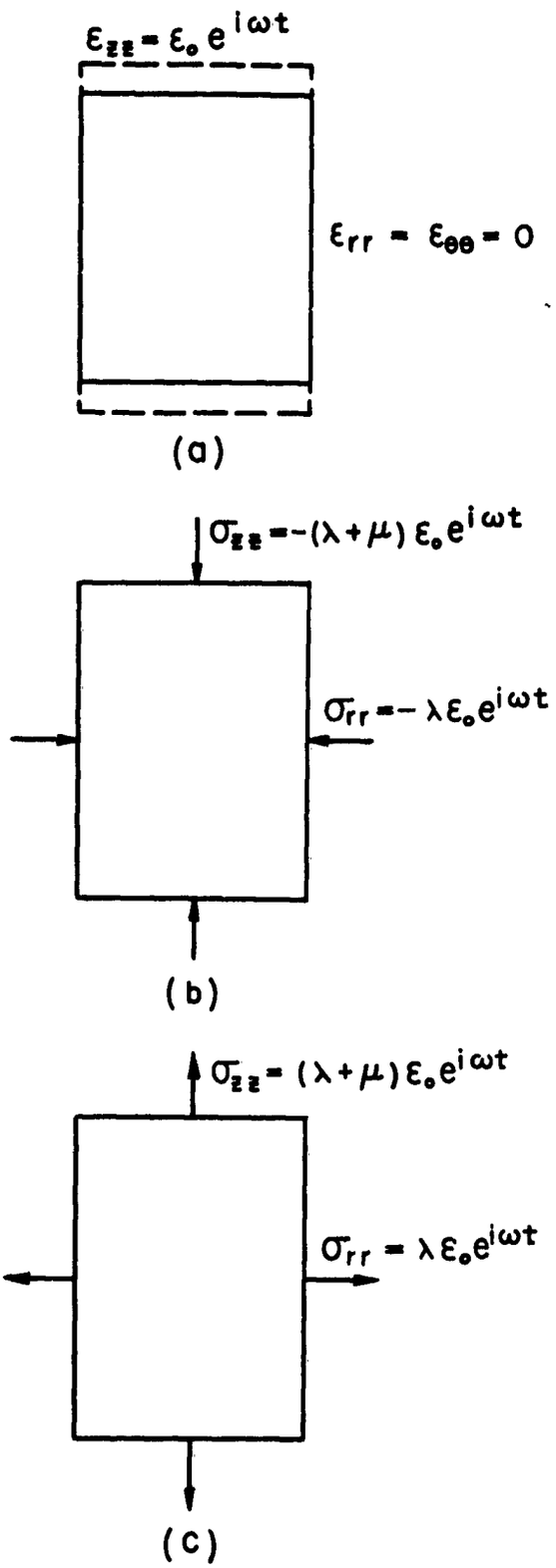

FIG. III-1 ILLUSTRATIVE PROBLEM

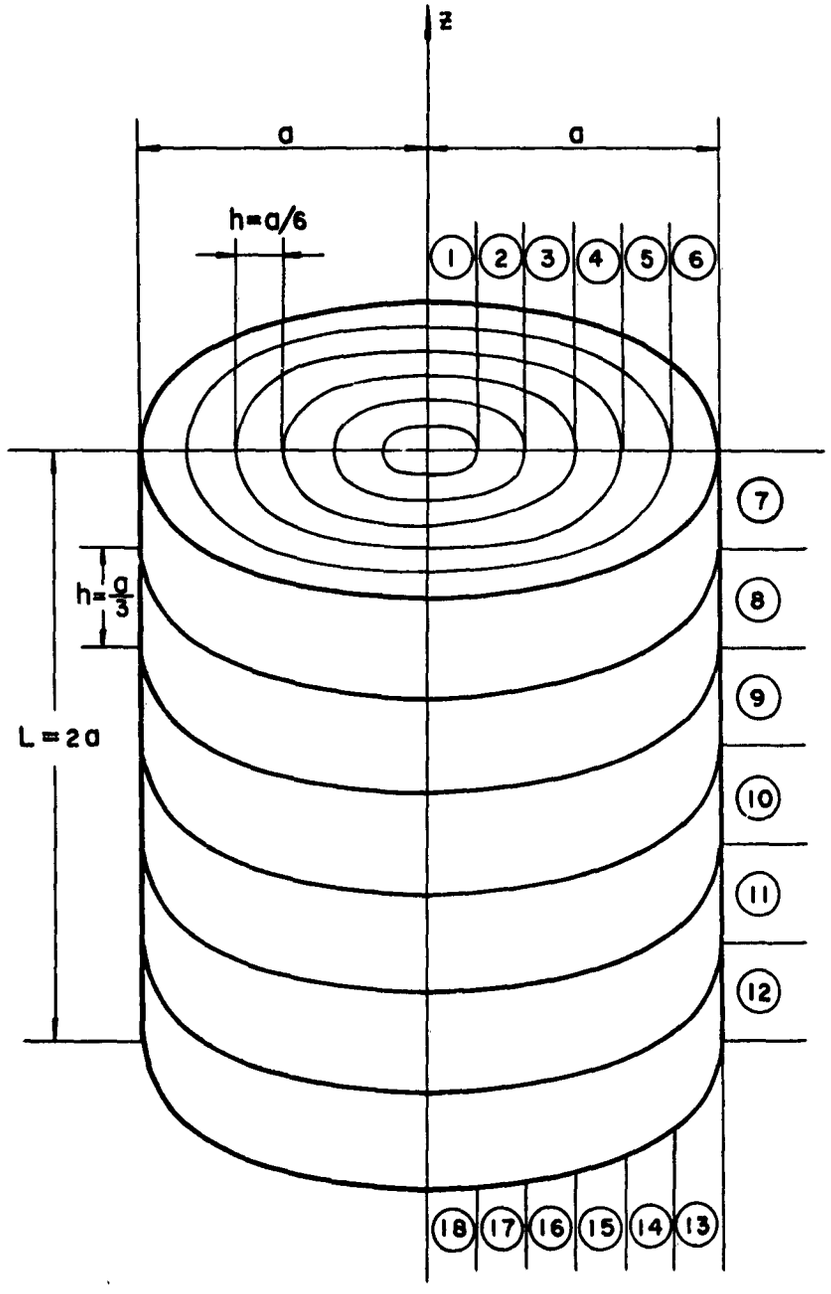

FIG. III-2 CYLINDER GEOMETRY

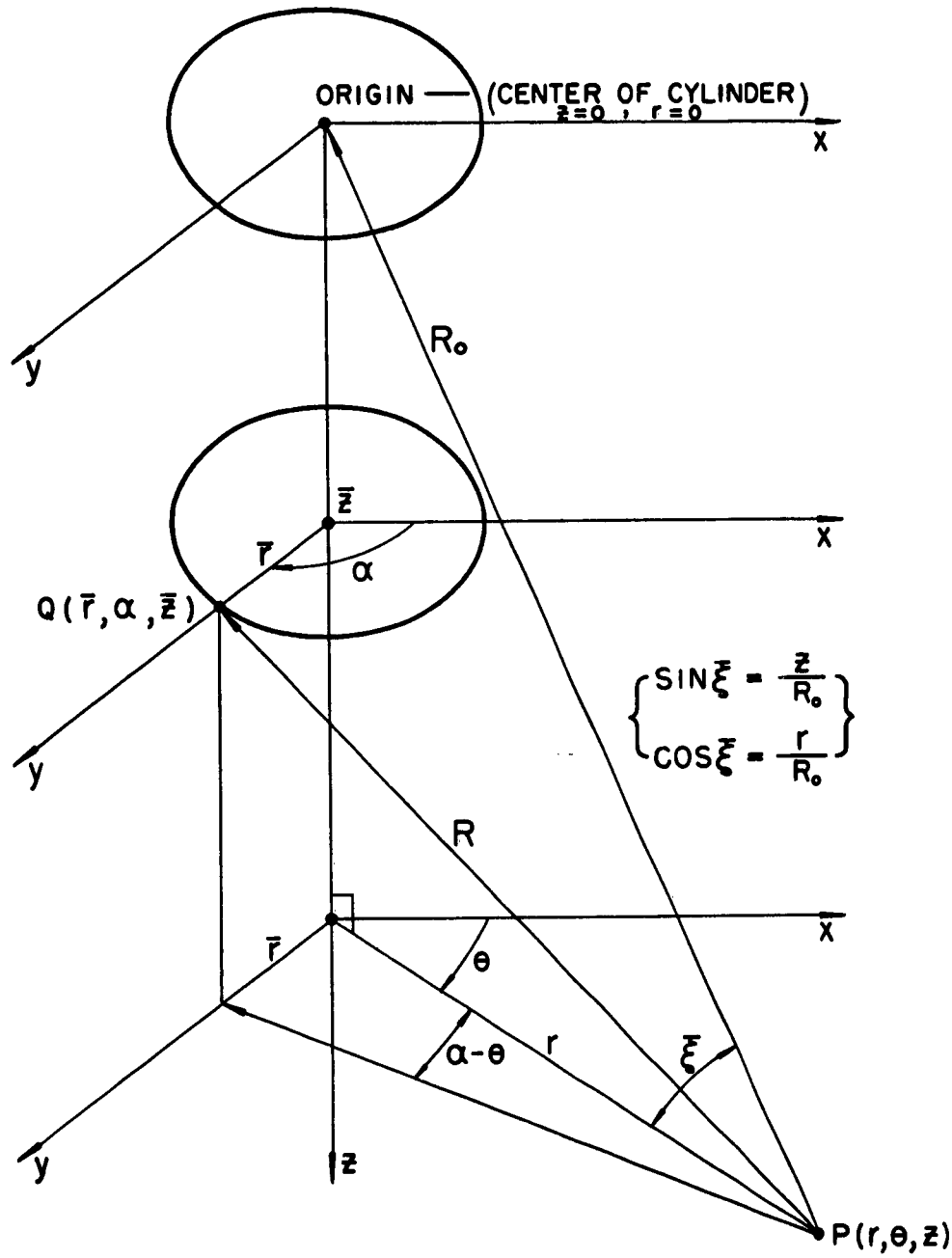

FIG. III-3 GEOMETRY FOR THE EVALUATION OF FLUID PRESSURES

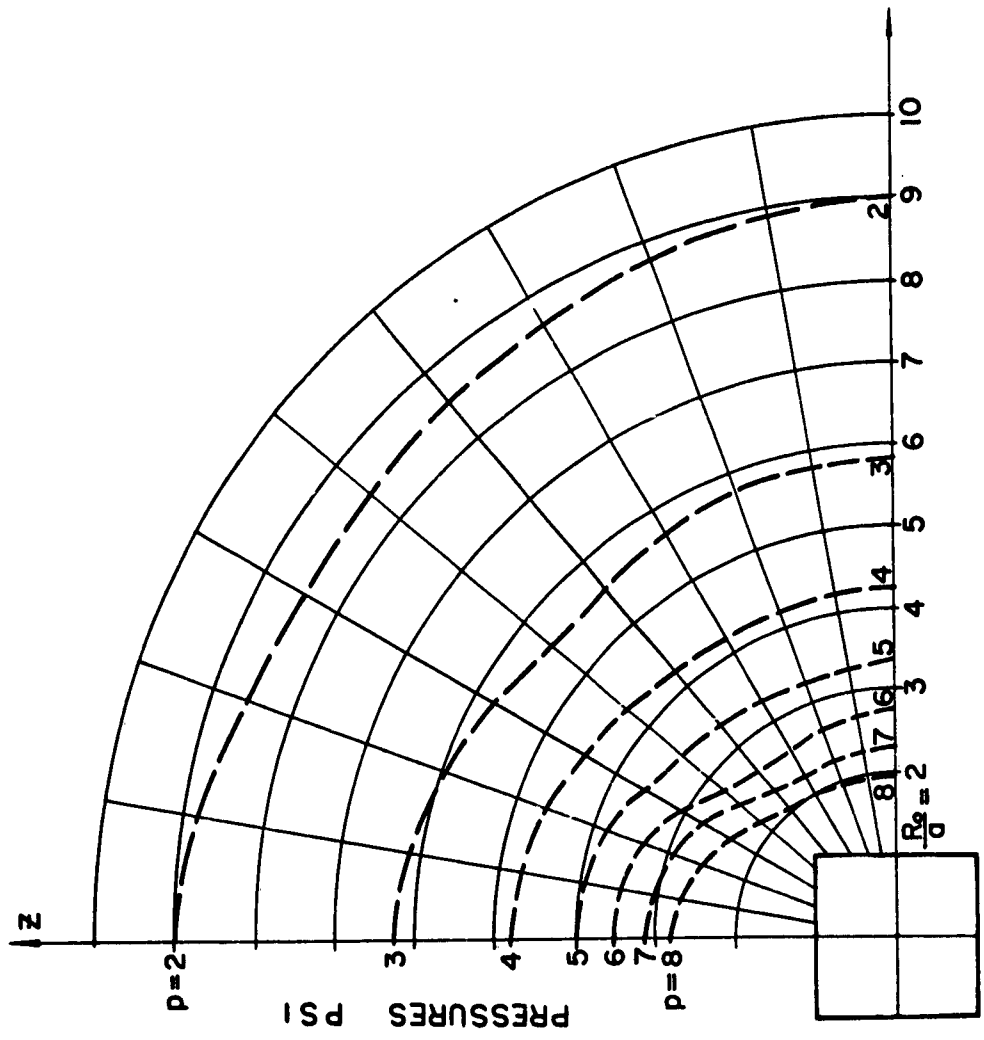

FIG III-4 FLUID PRESSURES; $R_o/a < 10$

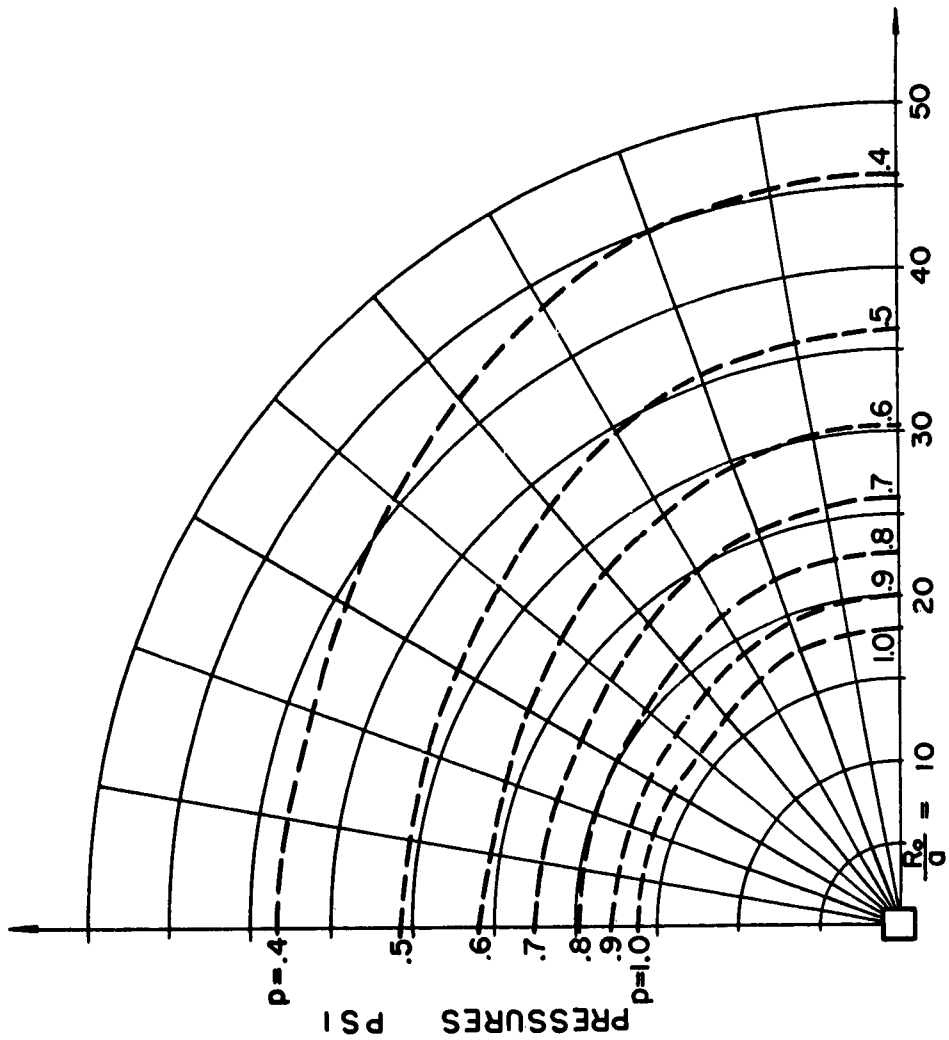

FIG. III-5 FLUID PRESSURES ; $R_o/a > 10$

APPENDIX A - EVALUATION OF THE REAL AND IMAGINARY PORTIONS OF THE COEFFICIENTS α_{nji} , β_{nji} , γ_{nji} AND THEIR SPACE DERIVATIVES.

For computational purposes, the complex coefficients α_{nji} , β_{nji} , γ_{nji} are written in terms of their real and imaginary parts, e.g.

$$\alpha_{nji} = \bar{\alpha}_{nji} + i\,\bar{\bar{\alpha}}_{nji} \tag{A-1}$$

The following nomenclature which is similar to that used in Appendix B of Reference [1] for the case n = 0, is used in this Appendix:

$$R = [(z-\bar{z})^2 + \bar{r}^2 + r^2 - 2r\bar{r}\cos\psi]^{\frac{1}{2}} \tag{A-2}$$

$$\bar{k}_\ell = \frac{\omega a}{c_\ell} \quad ; \quad \ell = 1,2,3 \tag{A-3}$$

$$X = k_\ell R = \bar{k}_\ell\,[(\xi-\bar{\xi})^2 + \bar{\rho}^2 + \rho^2 - 2\rho\bar{\rho}\cos\psi]^{\frac{1}{2}} \tag{A-4}$$

where

$$\xi = \frac{z}{a} \; ; \quad \bar{\xi} = \frac{\bar{z}}{a} \; ; \quad \rho = \frac{r}{a} \text{ and } \bar{\rho} = \frac{\bar{r}}{a} \tag{A-5}$$

Specific equations for the coefficients $\bar{\alpha}_{nji}$, $\bar{\bar{\alpha}}_{nji}$ and their space derivatives will be given in the Appendix. The corresponding expressions for the coefficients β_{nji} and γ_{nji} and their derivatives are obtained by replacing $\bar{k}_1 = \frac{\omega a}{c_1}$ with $\bar{k}_2 = \frac{\omega a}{c_2}$ (for β_{nji}) or $\bar{k}_3 = \frac{\omega a}{c}$ (for γ_{nji}) respectively in the equations which follow.

Real Part $\bar{\alpha}_{nji}$ of Coefficient α_{nji} and Derivatives

a) $i \neq j$

$$\bar{\alpha}_{nji} = -\frac{\bar{k}_1\bar{\rho}}{2\pi}\int_0^{\pi} \frac{\cos X}{X} \cos n\psi \, d\psi \tag{A-6}$$

$$a\bar{\alpha}^r_{nji} = \frac{\bar{k}_1^3\bar{\rho}}{2\pi}\int_0^{\pi} (\rho-\bar{\rho}\cos\psi)\bar{F}_1(\psi) \cos n\psi \, d\psi \tag{A-7}$$

$$a\bar{\alpha}^z_{nji} = \frac{\bar{k}_1^3\bar{\rho}}{2\pi}\int_0^{\pi} (\xi-\bar{\xi})\bar{F}_1(\psi) \cos n\psi \, d\psi \tag{A-8}$$

$$a^2\bar{\alpha}^{rr}_{nji} = \frac{\bar{k}_1^3\bar{\rho}}{2\pi}\int_0^{\pi} [\bar{F}_1(\psi)+(\rho-\bar{\rho}\cos\psi)^2\bar{F}_2(\psi)] \cos n\psi \, d\psi \tag{A-9}$$

$$a^2\bar{\alpha}^{zz}_{nji} = \frac{\bar{k}_1^3\bar{\rho}}{2\pi}\int_0^{\pi} [\bar{F}_1(\psi)+(\xi-\bar{\xi})^2\bar{F}_2(\psi)] \cos n\psi \, d\psi \tag{A-10}$$

$$a^3\bar{\alpha}^{zzz}_{nji} = \frac{\bar{k}_1^5\bar{\rho}}{2\pi}\int_0^{\pi} [3(\xi-\bar{\xi})\bar{F}_2(\psi)+(\xi-\bar{\xi})^3\bar{F}_3(\psi)] \cos n\psi \, d\psi \tag{A-11}$$

$$a^2\bar{\alpha}^{rz}_{nji} = \frac{\bar{k}_1^5\bar{\rho}}{2\pi}\int_0^{\pi} (\rho-\bar{\rho}\cos\psi)(\xi-\bar{\xi})\bar{F}_2(\psi)\cos n\psi \, d\psi \tag{A-12}$$

$$a^3\bar{\alpha}^{zrr}_{nji} = \frac{\bar{k}_1^5\bar{\rho}}{2\pi}\int_0^{\pi} [(\xi-\bar{\xi})\bar{F}_2(\psi)+(\xi-\bar{\xi})(\rho-\bar{\rho}\cos\psi)^2\bar{F}_3(\psi)] \cos n\psi \, d\psi \tag{A-13}$$

$$a^3\bar{\alpha}^{rzz}_{nji} = \frac{k_1^5\bar{\rho}}{2\pi}\int_0^{\pi} [(\rho-\bar{\rho}\cos\psi)\bar{F}_2(\psi)+(\ell-\bar{\ell})^2(\rho-\bar{\rho}\cos\psi)\bar{F}_3(\psi)]\cos n\psi\, d\psi \quad (A\text{-}14)$$

where

$$\bar{F}_1(\psi) = \frac{X\sin X + \cos X}{X^3} \quad (A\text{-}15)$$

$$\bar{F}_2(\psi) = \left[\frac{(X^2-3)\cos X - 3X\sin X}{X^5}\right] \quad (A\text{-}16)$$

$$\bar{F}_3(\psi) = \left[\frac{(15-6X^2)\cos X + (15-X^2)\,X\sin X}{X^7}\right] \quad (A\text{-}17)$$

b) $\underline{i = j}$

For the case i = j, i.e. where the field points and the source points lie on the same band, special formulas are required for the computation of α_{nii}, β_{nii}, γ_{nii} and their space derivatives. The reader is referred to Appendix C of Reference [1] for the derivation of these expressions for the case n = 0. The corresponding formulas for n ≠ 0 are given below.

$$\bar{\alpha}_{nii} = -\frac{\bar{k}\bar{\rho}}{2\pi}\int_0^{\pi}\frac{\cos X}{X}\cos n\psi + \lambda a\left[-\frac{\sin\left(\frac{\bar{k}\bar{a}}{a}\right)}{2\bar{k}}\right] \tag{A-18}$$

$$a\bar{\alpha}^{r}_{nii} = \frac{\bar{k}^3\bar{\rho}}{2\pi}\int_0^{\pi}(\rho-\bar{\rho}\cos\psi)\,\bar{F}_1(\psi)\cos n\psi\,d\psi \qquad j \text{ on surfaces } z=0,L$$

$$\frac{\bar{k}^3\bar{\rho}}{2\pi}\int_0^{\pi}(\rho-\bar{\rho}\cos\psi)\,\bar{F}_1(\psi)\cos n\psi\,d\psi + \frac{\lambda a}{2} \qquad j \text{ on surface } r=a \tag{A-19}$$

$$a\bar{\alpha}^{z}_{nii} = \frac{\lambda a}{2} \qquad j \text{ on surfaces } z=0,L$$

$$0 \qquad j \text{ on surface } r=a \tag{A-20}$$

$$a^2\bar{\alpha}^{rr}_{nii} = \frac{\bar{k}^3\bar{\rho}}{2\pi}\int_0^{\pi}[\bar{F}_1(\psi) + \bar{k}^2(\rho-\bar{\rho}\cos\psi)^2\,\bar{F}_2(\psi)]\cos n\psi\,d\psi + \lambda a\left[-\frac{\cos\left(\frac{\bar{k}\bar{a}}{a}\right)}{2\frac{\bar{a}}{a}}\right] \qquad j \text{ on surface } r=a \tag{A-21}$$

$$a^2\bar{a}^{zz}_{nii} = \frac{k^3\bar{\rho}}{2\pi}\int_0^{\pi} \mathbb{F}_1(\psi)\cos n\psi\, d\psi + \lambda a\left[-\frac{\cos\left(\frac{k\bar{a}}{a}\right)}{2\frac{\bar{a}}{a}}\right] \qquad j \text{ on surfaces } z=0,L \qquad \text{(A-22)}$$

$$a^3\bar{a}^{zzz}_{nii} = \lambda a\left[-\frac{k^2}{2}\right] \qquad j \text{ on surfaces } z=0,L \qquad \text{(A-23)}$$

$$a^2\bar{a}^{rz}_{nii} = 0 \qquad j \text{ on all surfaces} \qquad \text{(A-24)}$$

$$a^3\bar{a}^{zrr}_{nii} = 0 \qquad j \text{ on all surfaces} \qquad \text{(A-25)}$$

$$a^3\bar{a}^{rzz}_{nii} = \frac{k^5\bar{\rho}}{2\pi}\int_0^{\pi} [\rho-\bar{\rho}\cos\psi]\,\mathbb{F}_2(\psi)\cos n\psi\, d\psi \qquad j \text{ on all surfaces} \qquad \text{(A-26)}$$

Imaginary Part $\bar{\bar{\alpha}}_{nji}$ of Coefficient α_{nji} and Derivatives.

c) For all combinations of i and j.

$$\bar{\bar{\alpha}}_{nji} = \frac{\bar{k}_1\bar{\rho}}{2\pi}\int_0^{\pi} \frac{\sin X}{X} \cos n\psi \, d\psi \tag{A-27}$$

$$a\bar{\bar{\alpha}}^{r}_{nji} = \frac{\bar{k}_1^3\bar{\rho}}{2\pi}\int_0^{\pi} (\rho-\bar{\rho}\cos\psi)\,\bar{\bar{F}}_1(\psi)\cos n\psi \, d\psi \tag{A-28}$$

$$a\bar{\bar{\alpha}}^{z}_{nji} = \frac{\bar{k}_1^3\bar{\rho}}{2\pi}\int_0^{\pi} (\xi-\bar{\xi})\,\bar{\bar{F}}_1(\psi)\cos n\psi \, d\psi \tag{A-29}$$

$$a^2\bar{\bar{\alpha}}^{rr}_{nji} = \frac{\bar{k}_1^3\bar{\rho}}{2\pi}\int_0^{\pi} [\bar{\bar{F}}_1(\psi) + (\rho-\bar{\rho}\cos\psi)^2\,\bar{\bar{F}}_2(\psi)]\cos n\psi \, d\psi \tag{A-30}$$

$$a^2\bar{\bar{\alpha}}^{zz}_{nji} = \frac{\bar{k}_1^3\bar{\rho}}{2\pi}\int_0^{\pi} [\bar{\bar{F}}_1(\psi) + (\xi-\bar{\xi})^2\,\bar{\bar{F}}_2(\psi)]\cos n\psi \, d\psi \tag{A-31}$$

$$a^3\bar{\bar{\alpha}}^{zzz}_{nji} = \frac{\bar{k}_1^5\bar{\rho}}{2\pi}\int_0^{\pi} [3(\xi-\bar{\xi})\,\bar{\bar{F}}_2(\psi) + (\xi-\bar{\xi})^3\,\bar{\bar{F}}_3(\psi)]\cos n\psi \, d\psi \tag{A-32}$$

$$a^2\bar{\bar{\alpha}}^{rz}_{nji} = \frac{\bar{k}_1^5\bar{\rho}}{2\pi}\int_0^{\pi} (\rho-\bar{\rho}\cos\psi)(\xi-\bar{\xi})\,\bar{\bar{F}}_2(\psi)\cos n\psi \, d\psi \tag{A-33}$$

$$a^3\bar{\bar{\alpha}}^{zrr}_{nji} = \frac{\bar{k}_1^5\bar{\rho}}{2\pi}\int_0^{\pi} [(\xi-\bar{\xi})\,\bar{\bar{F}}_2(\psi) + (\xi-\bar{\xi})(\rho-\bar{\rho}\cos\psi)^2\,\bar{\bar{F}}_3(\psi)]\cos n\psi \, d\psi \tag{A-34}$$

$$a^3\bar{\bar{\alpha}}^{rzz}_{nji} = \frac{\bar{k}_1^5\rho}{2\pi}\int_0^{\pi}[(\rho-\bar{\rho}\cos\psi)\,\bar{\bar{F}}_2(\psi) + (\xi-\bar{\xi})^2(\rho-\bar{\rho}\cos\psi)\,\bar{\bar{F}}_3(\psi)]\cos n\psi\, d\psi \qquad \text{(A-35)}$$

where

$$\bar{\bar{F}}_1(\psi) = \begin{cases} -\frac{1}{3} + \frac{X^2}{20} - \frac{X^4}{840} \cdots & X < 0.06 \\ \left[\frac{X\cos X - \sin X}{X^3}\right] \cdots & X \geq 0.06 \end{cases} \qquad \text{(A-36)}$$

$$\bar{\bar{F}}_2(\psi) = \begin{cases} \frac{1}{15} - \frac{X^2}{210} + \frac{X^4}{7560} \cdots & X < 0.40 \\ \frac{(3-X^2)\sin X - 3X\cos X}{X^5} \cdots & X \geq 0.40 \end{cases} \qquad \text{(A-37)}$$

and

$$\bar{\bar{F}}_3(\psi) = \begin{cases} -\frac{1}{105} + \frac{X^2}{189} - \frac{X^4}{83,160} \cdots & X < 1.0 \\ \frac{(6X^2-15)\sin X + (15-X^2)X\cos X}{X^7} \cdots & X \geq 1.0 \end{cases} \qquad \text{(A-38)}$$

The quantities $\bar{\bar{\alpha}}_{nii}$, $\bar{\bar{\beta}}_{nii}$ and $\bar{\bar{\gamma}}_{nii}$ and their derivatives do not contain an infinite discontinuity in their integrands at the value defined by R = 0. Consequently, Eqs. (A-27)-(A-35) may be evaluated directly and there is no need for special formulas as in the case of the real (single barred) components.

APPENDIX B - DIAGRAMMATIC SUMMARY OF COMPUTATIONS.

The necessary computations for the evaluation of the pressure field in the fluid due to the time harmonic excitation of an elastic cylindrical body of finite length are summarized in Figs. (B-1) to (B-3). The computations are conveniently broken into three basic blocks as shown in the diagrams. The order of computations can, if necessary, be reorganized in accordance with the specific requirements of the particular electronic computer being used.

FIG. B-1 - DIAGRAMMATIC SUMMARY - BLOCK I.

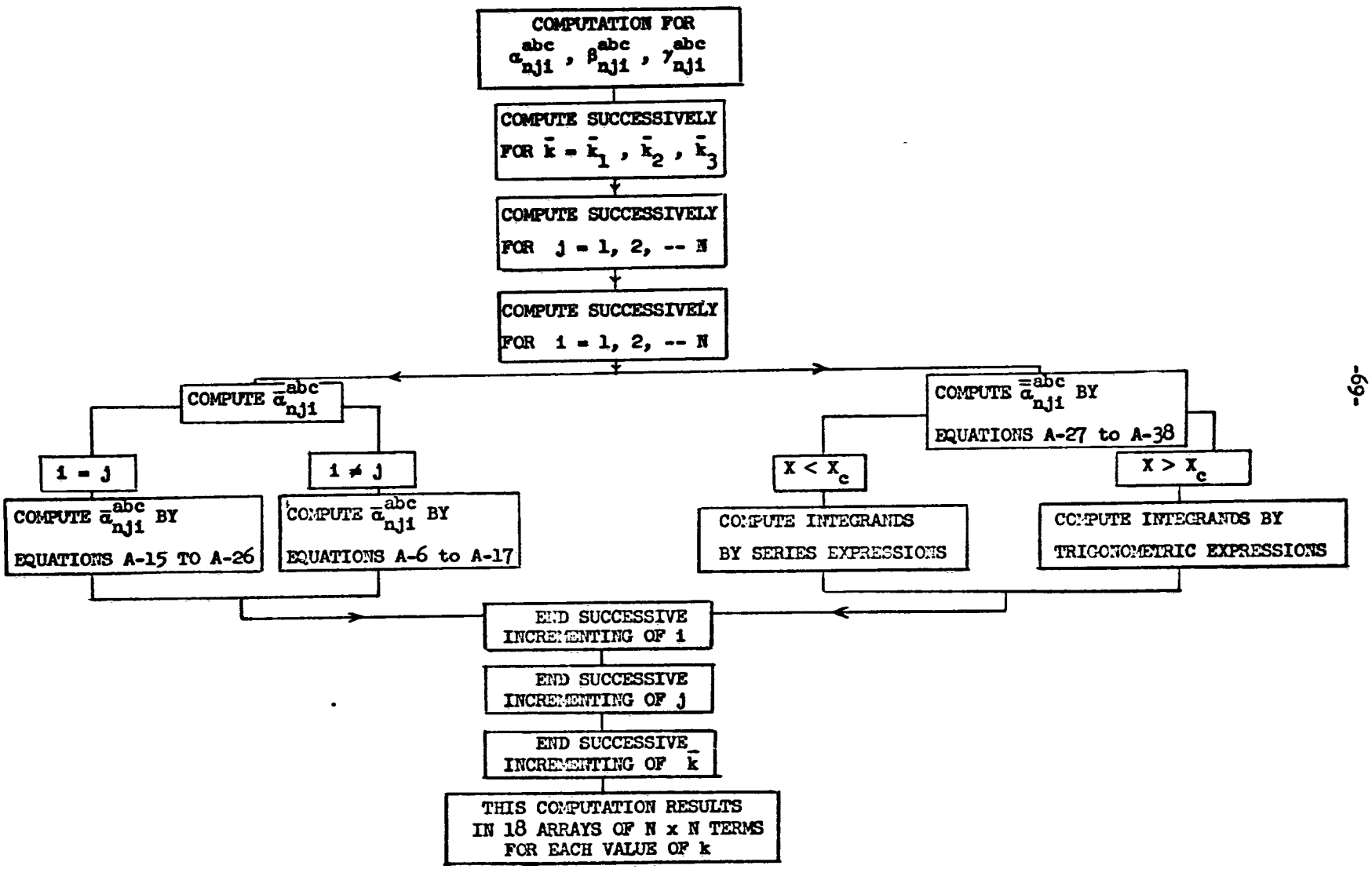

FIG. B-2 - DIAGRAMMATIC SUMMARY - BLOCK II.

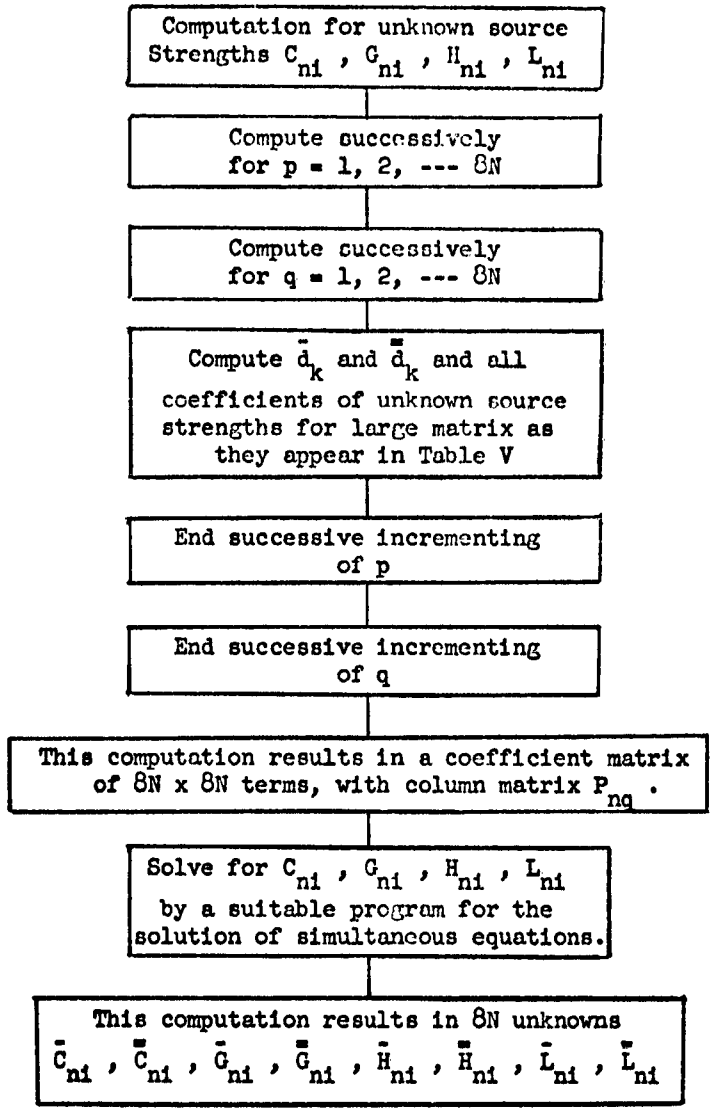

FIG. B-3 - DIAGRAMATIC SUMMARY - BLOCK III.

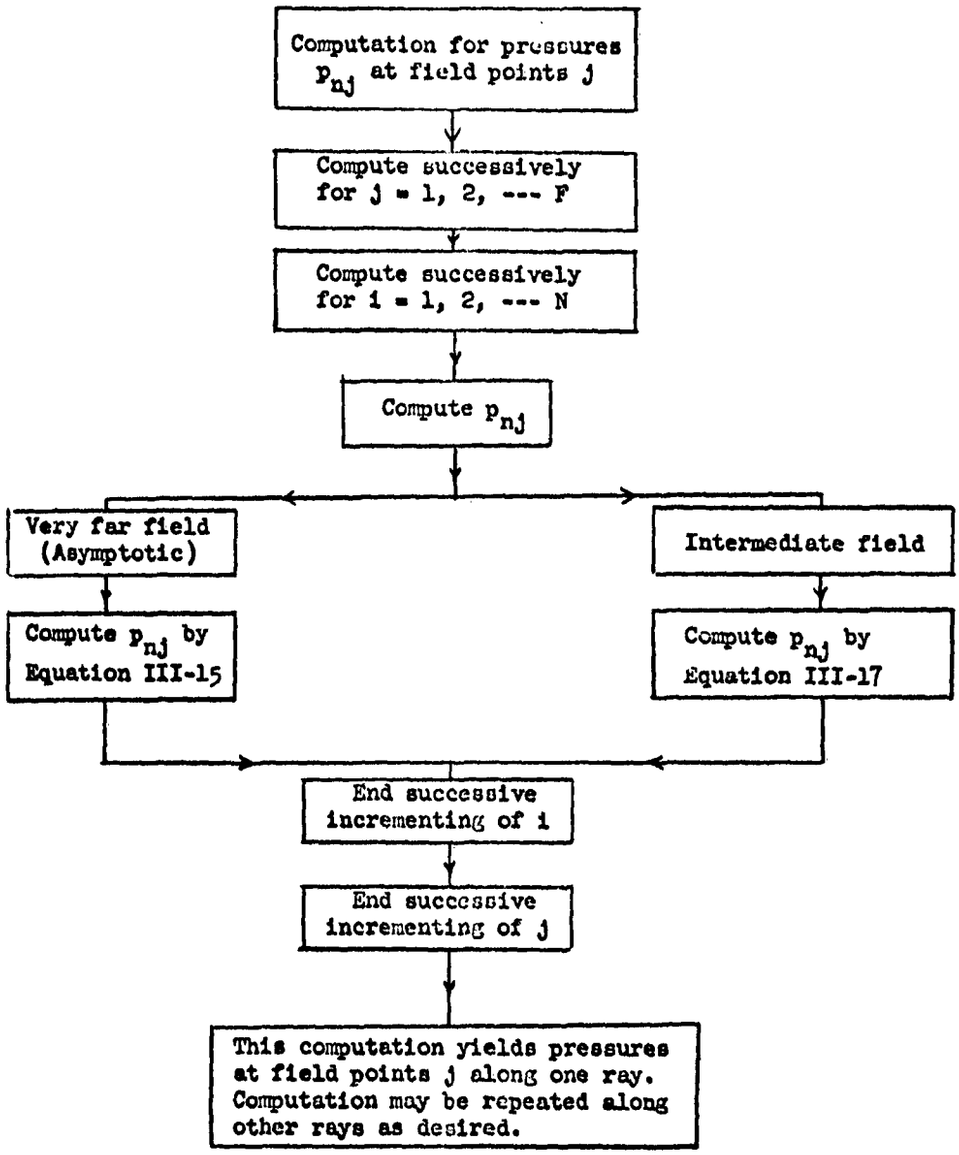

Distribution List

for

Unclassified Technical Reports Issued Under

Office of Naval Research Project NR-064-464, Contract Nonr-3454(00)FBM

SOUND IN STRUCTURES

NOTE: (1) Except as otherwise indicated below, forward one copy of all such reports to each of the following addressees.

(2) Separate mailing is required for each code where multiple codes are indicated.

A. Administrative & Liaison Activities

Chief of Naval Research
Department of the Navy
Washington 25, D.C.
Attn: Code 439 (2)
Code 468 (2)

Commanding Officer
Office of Naval Research
Branch Office
495 Summer Street
Boston 10, Massachusetts

Commanding Officer
Office of Naval Research
Branch Office
John Crerar Library Building
86 E. Randolph Street
Chicago 11, Illinois

Commanding Officer
Office of Naval Research
Branch Office
207 West 24th Street
New York 11, New York

Commanding Officer
Office of Naval Research
Branch Office
Navy #100, Fleet Post Office
New York, New York (5)

Director
Naval Research Laboratory
Washington 25, D.C.
Attn: Code 2000, Tech Info Of. (6)
Code 6200, Mechs Div.
Code 6250, Shock & Vibration
Code 6260, Structures
Code 5500, Sound Division

Armed Services Technical Information
Agency
Arlington Hall Station
Arlington 12, Virginia (10)

Office of Technical Services
Department of Commerce
Washington 25, D.C.

B. Members POLARIS Committee

Office of Naval Research
Department of the Navy
Washington 25, D.C.
Attn: Dr. F.J. Weyl, Code 102

Applied Physics Laboratory
John Hopkins University
8621 Georgia Avenue
Silver Spring, Maryland
Attn: Dr. W.H. Avery

Naval Ordnance Laboratory
White Oak
Silver Spring, Maryland
Attn: Dr. D.F. Bleil

U.S. Naval Electronics Laboratory
San Diego 52, California
Attn: Dr. R.J. Christensen

Chief
Bureau of Ships
Department of the Navy
Washington 25, D.C.
Attn: Capt. W.H. Cross, Code 403

Woods Hole Oceanographic Institute
Woods Hole, Massachusetts
Attn: Dr. P.M. Fye

Chief
Bureau of Naval Weapons
Department of the Navy
Washington 25, D.C.
Attn: Dr. E.S. Lamar, CR-12

U.S. Naval Ordnance Test Station
China Lake, California
Attn: Dr. T. Phipps

Office of Naval Research
Department of the Navy
Washington 25, D.C.
Attn: Capt. W.T. Sawyer, Code 406

Chief, Bureau of Ships
Department of the Navy
Washington 25, D.C.
Attn: Dr. G. Sponsler, Code 315

Director
Naval Research Laboratory
Department of the Navy
Washington 25, D.C.
Attn: Mr. P. Waterman, Code 5360

Missile & Space Division
Lockheed Aircraft Corporation
Palo Alto, California
Attn: Dr. W.F. Whitmore

Special Projects Office
(SP-114)
Bureau of Naval Weapons
Department of the Navy
Washington 25, D.C.
Attn: LCDR R.H. Yerbury
(Executive Secretary)

C. Department of Defense

Director of Defense Research
and Engineering
The Pentagon
Washington 25, D.C.
Attn: Technical Library

Chief, Defense Atomic Support
Agency
The Pentagon
Washington 25, D.C.
Attn: Tech. Info. Division
Blast & Shock Branch

D. Army

Office of the Secretary of the Army
The Pentagon
Washington 25, D.C.
Attn: Army Library

Chief of Staff
Department of the Army
Washington 25, D.C.
Attn: R & D Division

Office of the Chief of Engineers
Department of the Army
Washington 25, D.C.
Attn: ENG-HL Lib.Br., Adm. Ser.
ENG-NB Special Engr. Br., R&D Div.

Commanding Officer
Engineer Research Development Laboratory
Fort Belvoir, Virginia

Commanding Officer
Watertown Arsenal
Watertown, Massachusetts
Attn: Laboratory Division

Commanding Officer
Frankford Arsenal
Bridesburg Station
Philadelphia 37, Pennsylvania
Attn: Laboratory Division

U.S. Army Research Office
2127 Myrtle Drive
Duke Station
Durham, North Carolina
Attn: Div. of Engrg. Sciences

E. Navy

Chief of Naval Operations
Department of the Navy
Washington 25, D.C.
Attn: Op 07T

Commandant, Marine Corps
Headquarters, U.S. Marine Corps
Washington 25, D.C.

Commanding Officer
USNNOEU
Kirtland Air Force Base
Albuquerque, New Mexico
Attn: Code 20 (Dr. J.N. Brennen)

Chief, Bureau of Ships
Department of the Navy
Washington 25, D.C.
Attn: Code 335, Tech. Info. Div.
Code 345, Mr. F. Vane
Code 420
Code 421
Code 423
Code 425
Code 440
Code 442
Code 443
Code 689, Mr. I. Cook
Code 1500

Chief, Bureau of Naval Weapons
Department of the Navy
Washington 25, D.C.
Attn: RAAD, Airframe Design
DLI-3, Tech. Library
R-12, Chief Scientist
RMMA, MG & Airframe Br.
RU, ASW Division
RRRE, Research Br.

Special Projects Office
Bureau of Nav. Weapons
Department of the Navy
Washington 25, D.C.
Attn: Code SP-001, Chief Scientist
Code SP-20, Tech. Director

Chief, Bureau of Yards & Docks
Department of the Navy
Washington 25, D.C.
Attn: Code 70, Research
Code D428 Tech. Library

Commanding Officer & Director
David Taylor Model Basin
Washington 7, D.C.
Attn: Code 108, Mr. R.T. McGoldrick
Code 108B, Dr. M. Strassberg
Code 140, Tech. Info. Div.
Code 538, Dr. F. Theilheimer
Code 563, Mr. A.O. Sykes
Code 700, Dr. A.H. Keil
Code 720, Mr. E.E. Johnson
Code 731, Mr. J.G. Pulos
Code 740, Dr. W.J. Sette
Code 760, Mr. E. Noonan
Code 761, Dr. E. Buchman
Code 771, Dr. R. Liebowitz

DTMB Underwater Explosion Res. Div.
Norfolk Naval Shipyard
Portsmouth, Virginia
Attn: Mr. D.S. Coben

Commander
U.S. Naval Ordnance Laboratory
White Oak, Maryland
Attn: HL, Technical Library
D, Technical Director
OU, Underwater Weapons
RA, Acoustics Division

Commanding Officer & Director
U.S. Navy Underwater Sound Laboratory
Fort Trumbull
New London, Connecticut

Commanding Officer
U.S. Naval Mine Defense Laboratory
Panama City, Florida

Commander
U.S. Naval Air Development Center
Johnsville, Pennsylvania

Director
U.S. Navy Underwater Sound
Reference Laboratory
Office of Naval Research
P.O. Box 8337
Orlando, Florida

Commanding Officer & Director
U.S. Navy Electronics Laboratory
San Diego 52, California

Commander
Portsmouth Naval Shipyard
Portsmouth, New Hampshire

Commander
Mare Island Naval Shipyard
Vallejo, California

Director, Materials Laboratory
New York Naval Shipyard
Brooklyn 1, New York

Officer-in-Charge
Naval Civil Engineering Research
& Evaluation Laboratory
U.S. Naval Construction
Battalion Center
Port Hueneme, California

Director
Naval Air Experiment Station
Naval Air Material Center
Naval Base
Philadelphia 12, Pennsylvania
Attn: Structures Laboratory

Officer-in-Charge
David Taylor Model Basin
Underwater Explosion Research Division
Norfolk Naval Shipyard
Portsmouth, Virginia
Attn: Dr. H.M. Schauer

Commander
U.S. Naval Proving Ground
Dahlgren, Virginia

Supervisor of Shipbuilding, USN
and Naval Inspector of Ordnance
General Dynamics Corporation
Electric Boat Division
Groton, Connecticut

Commander
Naval Ordnance Test Station
China Lake, California
Attn: Physics Division
Mechanics Division

Commanding Officer
Naval Ordnance Test Station
Underwater Ordnance Division
3202 E. Foothill Boulevard
Pasadena 8, California

Commanding Officer & Director
U.S. Naval Engineering Experi-
ment Station
Annapolis, Maryland

Superintendent
U.S. Naval Postgraduate School
Monterey, California

F. Air Force

Commander
Air Material Command
Wright-Patterson Air Force Base
Dayton, Ohio
Attn: MCREX-B
Structures Division

Commander, WADD
Wright-Patterson Air Force Base
Ohio
Attn: WWRC
WWRMDS
WWRMDD

Director of Intelligence
Headquarters, U.S. Air Force
Washington 25, D.C.
Attn: P.V. Branch (Air Targets Div)

Commander
Air Force Office of Scientific
Research
Washington 25, D.C.
Attn: Mechanics Division

G. Other Government Activities

U.S. Atomic Energy Commission
Washington 25, D.C.
Attn: Director of Research

Director
National Bureau of Standards
Washington 25, D.C.
Attn: Division of Mechanics

National Aeronautics & Space Adm.
1512 H Street, N.W.
Washington 25, D.C.
Attn: Chief, Div. of Research
Information

Director
National Aeronautics & Space Adm.
Langley Research Center
Langley Field, Virginia
Attn: Structures Division

H. Contractors and Others

Dr. M.L. Baron
Paul Weidlinger, Consulting Engineer
770 Lexington Avenue
New York 21, New York

Professor H.H. Bleich
Department of Civil Engineering
Columbia University
618 Mudd Building
New York 27, New York

Professor B.A. Boley
Department of Civil Engineering
Columbia University
618 Mudd Building
New York 27, New York

Dr. M.A. Brull
Engineering Mechanics Division
University of Pennsylvania
Philadelphia 4, Pennsylvania

Dr. F.L. DiMaggio
Dept. of Civil Engineering
Columbia University
618 Mudd Building
New York 27, New York

Professor D.C. Drucker
Division of Engineering
Brown University
Providence 12, Rhode Island

Dr. Ira Dyer
Bolt, Beranek & Newman, Inc.
50 Moveton Street
Cambridge 38, Massachusetts

Professor A.C. Eringen
Dept. of Aeronautical Engineering
Purdue University
Lafayette, Indiana

Professor J.N. Goodier
Department of Mechanical Engineering
Stanford University
Stanford, California

Dr. Josh E. Greenspon
J.G. Engineering Research Assoc.
3709 Callaway Avenue
Baltimore 15, Maryland

Professor Philip G. Hodge
Armour Research Foundation
10 West 35th Street
Chicago, Illinois

Professor Nicholas J. Hoff
Dept. of Aeronautical Engineering
Stanford University
Stanford, California

Dr. C.W. Horton
Defense Research Laboratory
University of Texas
Austin 12, Texas

Dr. M.C. Junger
Cambridge Acoustical Associates
129 Mount Auburn Street
Cambridge 38, Massachusetts

Professor Joseph Kempner
Dept. of Aeronautical Engineering
& Applied Mechanics
Polytechnic Institute of Brooklyn
333 Jay Street
Brooklyn 1, New York

Professor J.M. Klosner
Dept. of Aeronautical Engineering
& Applied Mechanics
Polytechnic Institute of Brooklyn
333 Jay Street
Brooklyn 1, New York

Professor E.H. Lee
Brown University
Division of Applied Mathematics
Providence 12, Rhode Island

Professor R.D. Mindlin
Dept. of Civil Engineering
Columbia University
618 Mudd Building
New York 27, New York

Professor P.M. Naghdi
University of California
College of Engineering
Berkeley 4, California

Professor N.M. Newmark, Head
Department of Civil Engineering
University of Illinois
Urbana, Illinois

Professor F. Pohle
Department of Mathematics
Adelphi College
Garden City, New York

Professor W. Prager, Chairman
Physical Sciences Council
Brown University
Providence 12, Rhode Island

Professor F.V. Romano
Dept. of Aeronautical Engineering
& Applied Mechanics
Polytechnic Institute of Brooklyn
333 Jay Street
Brooklyn 1, New York

Professor E. Reiss
Institute of Mathematical Sciences
New York University
25 Waverly Place
New York 3, New York

Dr. V.L. Salerno
Don Bosco Institute for Research
Ramsey, New Jersey.

Professor A.S. Veletsos
Department of Civil Engineering
University of Illinois
Urbana, Illinois

Brown University
Research Analysis Group
Providence, Rhode Island

Electro Nuclear Systems Corporation
Technical Research Division
8001 Norfolk Avenue
Bethesda 14, Maryland

Hudson Laboratories
Columbia University
145 Palisades Street
Dobbs Ferry, New York

Lamont Geological Observatory
Columbia University
Torre Cliffs
Palisades, New York

Ordnance Research Laboratory
University of Pennsylvania
University Park, Pennsylvania

Woods Hole Oceanographic Institution
Woods Hole, Massachusetts

Issuing Contractor's Files (7)